CHAPTER 2

LIPID ANTIGEN IMMOBILISATION ON A BIOSENSOR SURFACE

2.1 Introduction

2.1.1 Biosensor technology

Antibody-antigen interactions are about molecular recognition. One way of characterising these interactions is to make use of biosensors. Biosensors are molecular sensors that detect and quantify molecular recognition by linking to a physical transduction technique to generate a measurable electronic signal that represents receptor-ligand interactions (qualitatively and/or quantitatively) in real-time (Cornell *et al.*, 1997; Thévenot *et al.*, 2001). Molecular recognition can be measured in complex biological samples as diverse as blood, urine, other bodily fluids and sewage effluent. Different types of biosensors exist, such as potentiometric (Reddy *et al.*, 2001), amperometric (Kulys & Vidziunaite, 2003), optic (Schneider *et al.*, 1997), conductimetric (Kim *et al.*, 2000), thermal (Ramanathan & Danielsson, 2001), acoustic (Barié & Rapp, 2001) and piezoelectric (Li *et al.*, 2002) biosensors. The resonant mirror biosensor (an optical biosensor) combines the simplicity and ease of use of surface plasmon resonance biosensors, with the improved sensitivity of wave-guide sensors (Cush *et al.*, 1993).

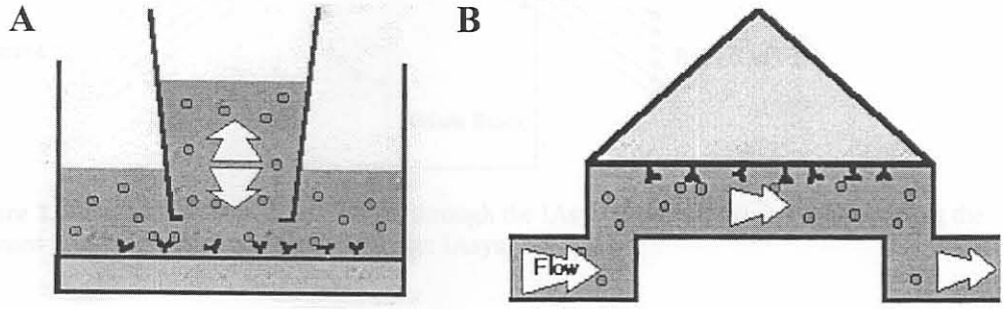

Figure 2.1: Two configurations of a molecular interaction chamber of a biosensor. **(A)** a micro cuvette or **(B)** a micro flow cell. (Source: http://www.cores.utah.edu/interaction/analyte.htm)

There are two different ways of introducing analyte in a sample to the ligand-coated sensor surface where the molecular recognition is to take place: a micro cuvette or a micro flow cell (Figure 2.1). Both types of systems have advantages and disadvantages, but the micro cuvette system is more appropriate for innovation and optimisation purposes due to easy access to the cuvette and the simplicity of the system (Nice & Catimel, 1999).

The IAsys Affinity Sensors system used in this study is a resonant mirror biosensor equipped with a binary cell (channel) micro cuvette system, allowing the comparison of two samples to one another. The cuvette is specially arranged to incorporate a prism through which laser light is projected from a moving source over a range of different angles. The laser light propagates through the prism and is reflected off the internal surfaces it encounters. At one specific angle, called the resonant angle, the light moves through the prism surface and into the layer next to the surface called the coupling layer (1000nm thick). Then it moves into the next layer called the resonant layer (100nm thick). The evanescent field is the region above the resonant layer where the electromagnetic field created by the laser light is affected by accumulation of ligates to the ligands (IAsys, 1995a, 1995b) (Figure 2.2). Accumulation or decrease of mass in the evanescent field alters the refractive index of the resonant structure, causing the resonant angle of the incident light to change. This change in angle is recorded in real-time by the IAsys software in arc seconds.

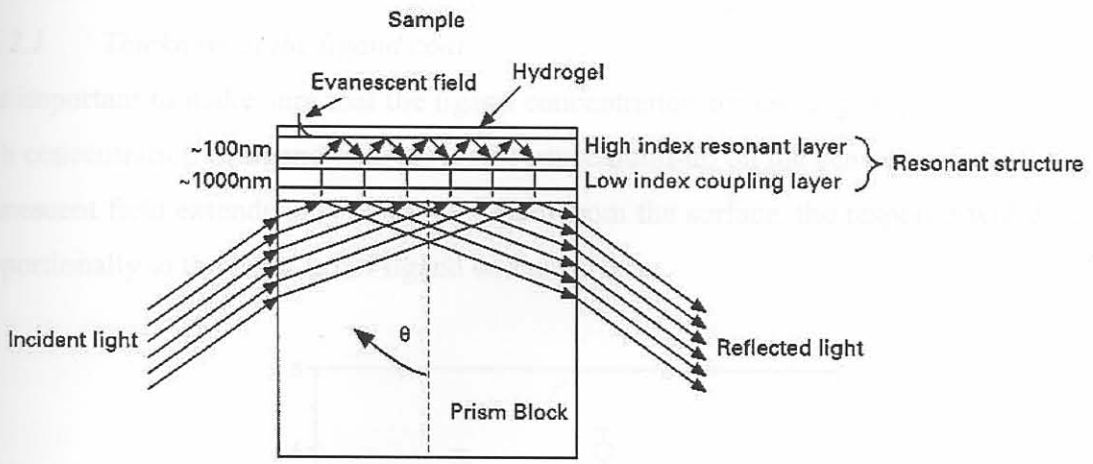

Figure 2.2: Optical pathway of laser light through the IAsys biosensor prism block showing the resonant layer and evanescent field. (Source: IAsys, 1995a)

The IAsys biosensor has twin internal aspirators that allow the removal of solutions from the cuvette cells without removing the cuvette from the biosensor. This expedites the pipetting of solutions. Integral stirrers ensure that the solutions are homogenous at all times and limit the effect of mass transfer through passive diffusion.

After chemical immobilisation of receptor molecules (ligands) to the sensor surface, the molecules specific for the receptors (ligates) can bind to the receptors. This interaction is called association and its strength is dependent on the affinity of the ligand for the ligate.

Displacement of the solution containing the ligate with buffer causes the ligate to dissociate from the ligands on the principle of diffusion from a higher to a lower concentration; this is called the dissociation phase. Because not all ligate molecules are removed during the dissociation phase the surface needs to be regenerated for another round of association/dissociation (IAsys 1995a, 1995b).

The system can be used for the determination of concentration, specificity of molecular recognition, kinetics of binding, co-operativity and quantitative parameters of association and dissociation interactions between ligand-ligate pairs (Nice & Catimel, 1999).

2.1.2 Practical considerations

During an interaction analysis, the factors that influence interactions must be considered. Because so much diversity exists in biomolecules, it is impossible to have a single protocol that will work for every sample.

2.1.2.1 Thickness of the ligand coat

It is important to make sure that the ligand concentration for coating is minimised. If a too high concentration of ligand is used, it will cause build-up on the sensor surface. Since the evanescent field extends only to about 100nm from the surface, the response will decrease proportionally to the build-up of ligand on the surface.

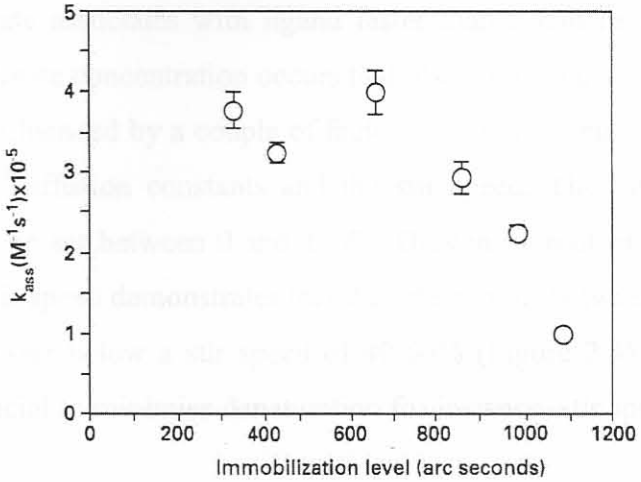

Figure 2.3: An example of the effect of ligand immobilisation level on the rate of association of a ligate on an IAsys biosensor CMD cuvette surface. (Source: IAsys, 1995b)

A plot of association constants versus mass of ligand immobilised demonstrates that this relationship is not linear, but that it plateaus already at low immobilisation levels and gradually loses responsivity (Figure 2.3). Therefore the ligand concentration should be optimised for immobilisation.

2.1.2.2 Type of cuvette surface

A variety of cuvette surfaces are available for different applications. In protein-protein interactions, a CMD surface is used most often as it provides an easy way to immobilise proteins onto the surface using EDC/NHS chemistry. However, sometimes the three-dimensional dextran surface might obstruct ligate molecules from associating with immobilised ligand molecules, thereby changing the kinetics of the sample. In cases where this is suspected, other types of surfaces can be used. Typically, carboxyl and aminosilane surfaces are used to orientate molecules in a specific way. An increasingly popular surface is the biotinylated surface that captures streptavidin-labelled molecules.

2.1.2.3 Mass transfer

Whenever a solution is flowing or moving over an adsorptive stationary layer, part of the mobile solution will also be stationary. In the biosensor, ligate must move through this 'unstirred' layer to associate with the ligand. The effect created by this movement is called mass transport. Under ideal conditions, ligate in the unstirred layer is replaced as soon as it is bound to the ligand, and also removed during dissociation before re-association can occur. But when ligate associates with ligand faster than it can be replaced, a transient lowering of surface ligate concentration occurs that also slows the association. These mass transfer effects are influenced by a couple of factors like kinetic rate constants, ligand and ligate concentration, diffusion constants and the stir speed. The integral stirrers of the IAsys biosensor can be set between 0 and 100%. Drawing a plot of the apparent on-rate (k_{on}) values versus stir speed demonstrates that the interactions between ligand and ligate is limited by mass transfer below a stir speed of 40-60% (Figure 2.4). Therefore, unless a slow stir speed is crucial to minimise denaturation for instance, stir speeds of 70%+ should be used.

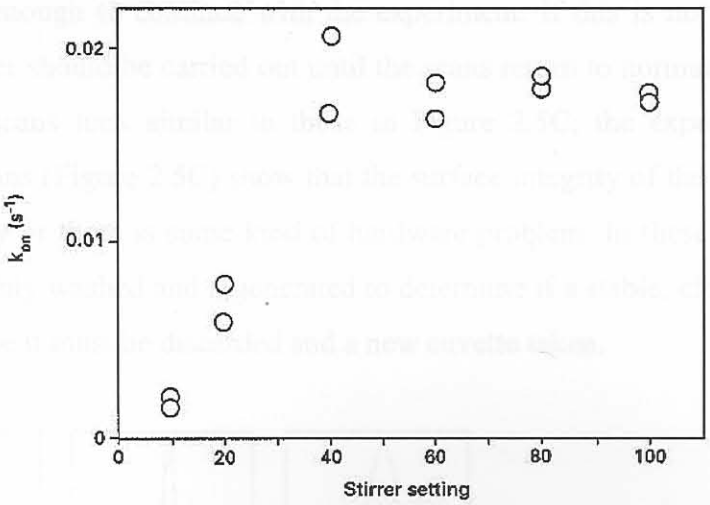

Figure 2.4: An example of the effect of stir speed on the apparent on-rate, k_{on}, of a ligate's association to a CMD surface immobilised ligand. (Source: IAsys, 1995b)

2.1.2.4 Regeneration

Using the same surface of immobilised ligand, it is possible to carry out a number of interaction analyses with different concentrations of ligate. Because dissociation is very seldom complete, the surface needs to be stripped of all the bound ligate and other non-specific impurities by a process of regeneration. Regeneration is done by adding a solution that lowers or increases the pH and thereby breaking the non-covalent interactions between the ligand and the ligate. Typical regeneration solutions are hydrochloric acid, formic acid, sodium carbonate or ethanol. Some regeneration buffers denature proteins under certain conditions, so care should be taken to optimise the regeneration solution type as well as concentration and pH.

2.1.2.5 Resonance scan diagnostics

A resonance scan is a measure of the integrity of the evanescent field and is a useful tool to determine the reliability of experimental data. It is important to note that the resonance scan profile will change during an experiment, especially during ligand immobilisation and regeneration when the structural composition at the surface changes most dramatically. It is important to take resonance scans during baseline events but also before and after immobilisation and between bindings. Normal scans are shown in Figure 2.5A. Scans that are sometimes obtained during an experiment that are also considered to be reasonable are shown in Figure 2.5B. Only when these scans return to smooth, defined peaks as in Figure 2.5A, during a phase where a stable surface is expected, can it be concluded that the

surface is stable enough to continue with the experiment. If this is not the case, washes with running buffer should be carried out until the scans return to normal. If this cannot be achieved or the scans look similar to those in Figure 2.5C, the experiment should be aborted. These scans (Figure 2.5C) show that the surface integrity of the cuvette is failing, the cuvette is dirty or there is some kind of hardware problem. In these cases the cuvette should be thoroughly washed and regenerated to determine if a stable, clean surface can be regained, otherwise it must be discarded and a new cuvette taken.

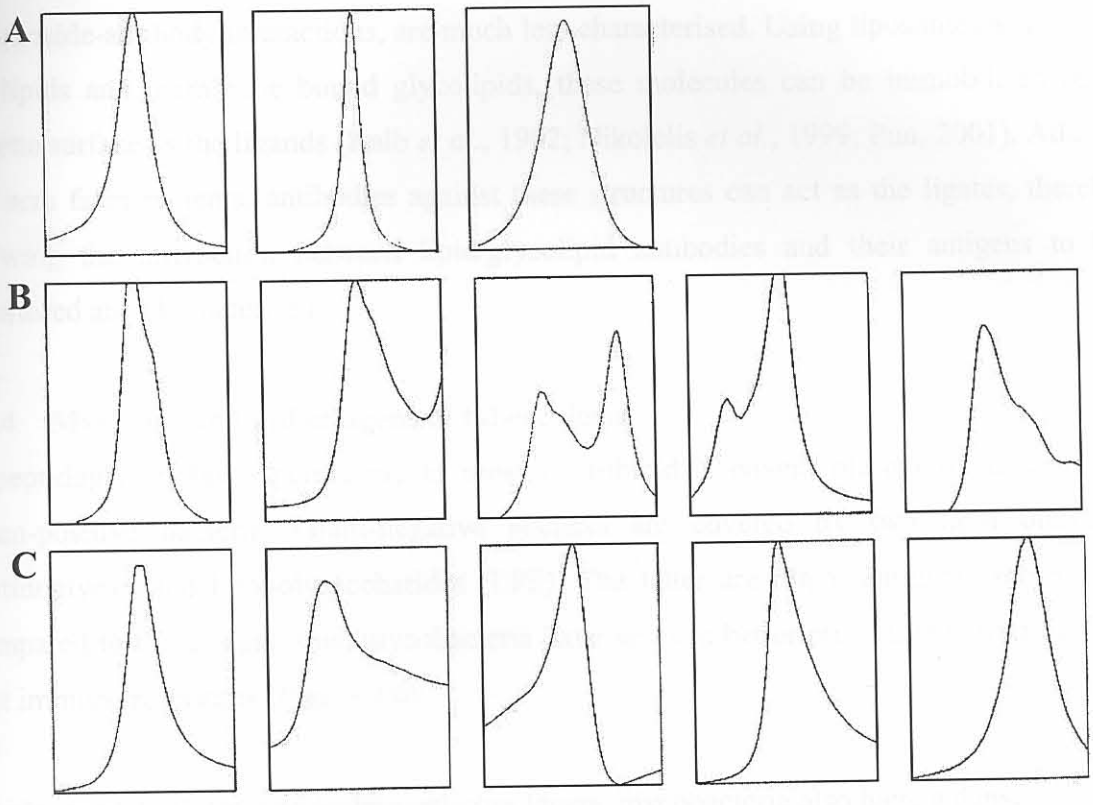

Figure 2.5: Examples of possible resonance scans of the IAsys biosensor cuvette surface obtained during an experiment that includes immobilisation, interaction analysis and regeneration. **(A)** Acceptable resonance scans obtained when the surface integrity is uniform and stable. **(B)** Resonance scans that may be seen when the surface is unstable. If these scans return to acceptable profiles during an expected stable event, the surface is still useful. **(C)** Abnormal resonance scans indicating dirty cuvettes or hardware problems. (Source: IAsys, 1995b)

2.1.2.6 Running buffer composition

All solutions have their own unique refractive indices that influence the angle of incidence light needed to obtain total internal reflection in the biosensor set-up. An important consequence is that the recorded response also change (abruptly) when solutions are exchanged in a biosensor cuvette. Accordingly, it is very important that the composition of running buffers used for test sample dilutions and wash steps during interaction analyses, be the same.

2.1.3 Biosensor applications in lipid-induced auto-immunity

The biosensor field is expanding rapidly. Protein-protein interactions were the first to be studied using a biosensor and are also the best characterised (Rubio *et al.*, 1997; Hirmo *et al.*, 1999; Altin *et al.*, 2001). Other interactions that have been tested before include DNA-protein, DNA-DNA hybridisation, carbohydrate-protein and even particulate interactions like cell-protein interactions (IAsys, 1995b; BIAcore, 2001).

Lipid-protein interactions such as MA-antibody, and glycolipid-protein interactions such as ganglioside-antibody interactions, are much less characterised. Using liposomes as carriers for lipids and membrane bound glycolipids, these molecules can be immobilised on a cuvette surface as the ligands (Kalb *et al.*, 1992; Nikolelis *et al.*, 1999; Puu, 2001). Adding test sera from patients, antibodies against these structures can act as the ligates, thereby allowing the interaction between lipid/glycolipid antibodies and their antigens to be monitored and characterised.

2.1.4 Mycolic acid lipid antigens in tuberculosis

A peptidoglycan layer permeable to most microbicidals covers plasma membranes of Gram-positive bacteria. Gram-negative bacteria are covered by two lipid bilayers, peptidoglycan and lipopolysaccharides (LPS). The latter are major antigenic molecules. Compared to these organisms, mycobacteria have an even better protective barrier against host immune responses (Figure 2.6).

Besides peptidoglycan and arabinogalactan layers, mycobacteria also have a dense layer of acyl lipids, lipoarabinomannan (LAM) and mycolates (MA). The cell envelope of *Mycobacterium* species consists of an outer capsule, a cell wall and a plasma membrane (Daffé & Draper, 1998). The cell wall, composed of MA arranged along with the acyl lipids in a bilayer, serves as a permeability barrier separate of the plasma membrane and is extremely low in fluidity (Liu *et al.*, 1996). Mycolic acids are α-alkyl, β-hydroxyl fatty acids of high molecular weight (C_{60}-C_{90}) and constitute 40-60% (mass %) of the complex cell envelope (Minnikin, 1982).

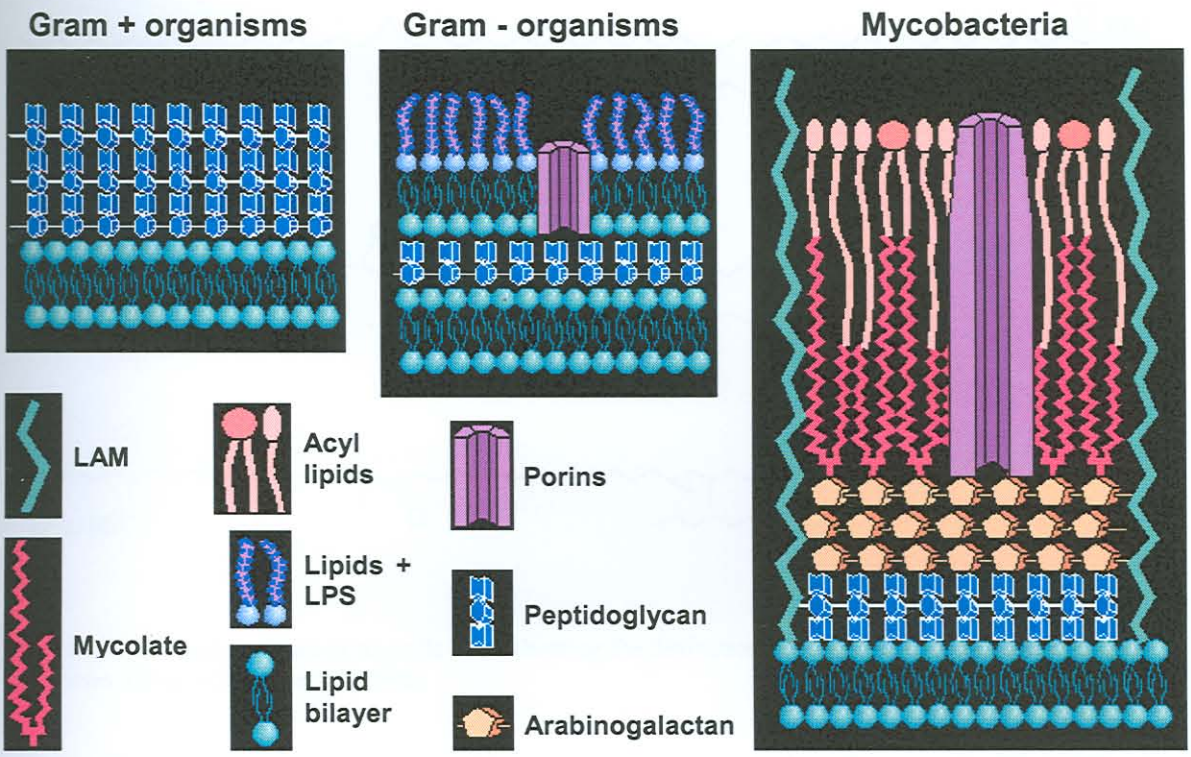

Figure 2.6: A comparison of bacterial cell barrier structures. Gram+ bacteria have only peptidoglycan besides a plasma membrane and Gram- bacteria have a double membrane with peptidoglycan and LPS. Mycobacteria have peptidoglycan and arabinogalactan layers that are covered by a bilayer consisting of MA and acyl lipids. LAM - lipoarabinomannan, LPS – lipopolysaccharides. (Source: Stannard, 1996)

Mycolic acids consist of mainly three subclasses: α-, keto- and methoxy-MA (Figure 2.7). In *Mycobacterium tuberculosis*, α-MA comprises almost half the total amount while the other two subclasses share the remainder almost equally (Barry *et al.*, 1998). It has been shown that only certain subclasses are responsible for MA's biological activity: one laboratory describes that antibodies against cord factor (trehalose 6,6'-dimycolate) recognises methoxy-MA stronger than the other subclasses (Pan *et al.*, 1999), while another shows that specifically the oxygenated MA (methoxy- and keto-) are responsible for *M. tuberculosis*' virulence in mice (Dubnau *et al.*, 2000).

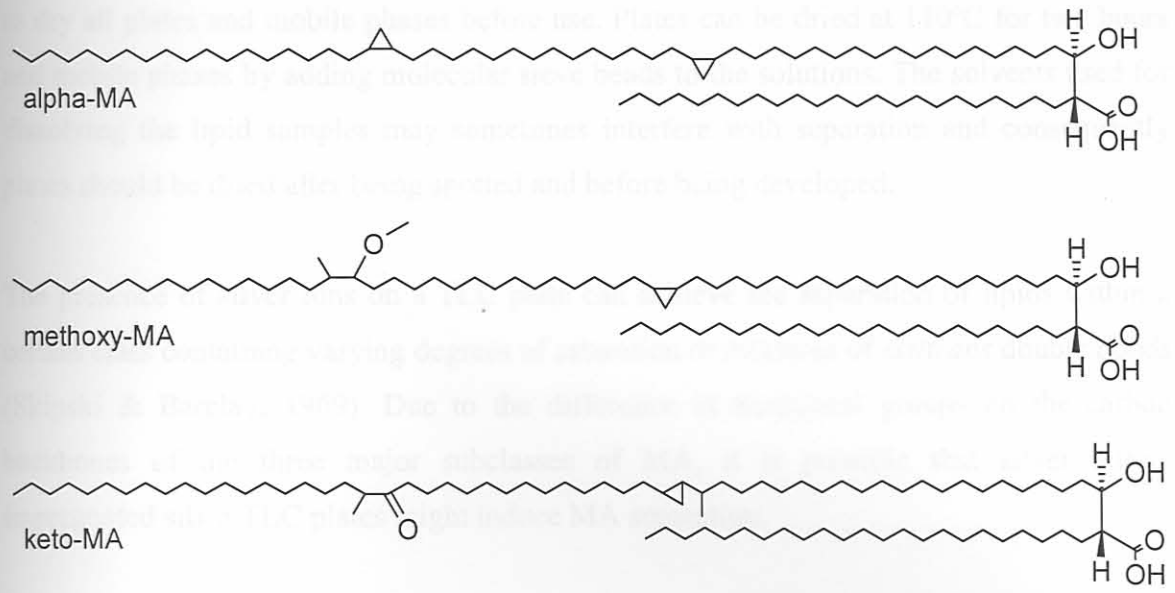

Figure 2.7: General structure of mycolic acids showing the distinction between the α-, keto- and methoxy-subclasses. (Source: Barry *et al.*, 1998)

As described in Chapter 1, an optical biosensor is well suited to characterise the interaction between antibodies and MA. Because the MA subclasses are not equally antigenic, it is preferable that the subclasses be characterised separately in the biosensor in terms of their antigenicity. Mycolic acid separation was achieved on preparative scale by Kaneda *et al.* (1986) using a silica column and on an analytical scale by Watanabe *et al.* (2001) using thin layer chromatography (TLC). Silica columns separate molecules on the same principle as silica TLC.

The separation of various lipids using TLC has been described in several articles (Dasgupta & Hogan, 2001; Kishimoto *et al.*, 2001; Wilson & Sargent, 2001) and reviewed in others (Skipski & Barclay, 1969; Olsson, 1992). The principle involves the application of small spots of lipid to a polar adsorbent immobilised onto a rigid support structure like aluminium or glass. The plates are placed upright in a tank containing a mobile phase usually consisting of organic solvents. Through capillary action, the mobile phase moves up through the adsorbent layer, dissolving the lipids in the spots along the way. The relative mobility of individual lipids is determined by the chemical groups, carbon chain length and isomerisation, thereby effecting a separation

A few aspects about lipid TLC are important to note: separation is affected by the presence of water both on the silica plate and in the organic mobile phase. Therefore it is important

to dry all plates and mobile phases before use. Plates can be dried at 110°C for two hours and mobile phases by adding molecular sieve beads to the solutions. The solvents used for dissolving the lipid samples may sometimes interfere with separation and consequently plates should be dried after being spotted and before being developed.

The presence of silver ions on a TLC plate can achieve the separation of lipids within a certain class containing varying degrees of saturation or mixtures of *cis*/*trans* double bonds (Skipski & Barclay, 1969). Due to the difference in functional groups on the carbon backbones of the three major subclasses of MA, it is possible that silver nitrate impregnated silica TLC plates might induce MA separation.

Lipids are not so easily detected, due to their lack of natural chromophores. Different detection methods are available: some specific for certain lipids or lipid classes, and some general for detecting most lipids. Mycolic acids are waxes and no specific detection method exists for visualising MA on developed TLC plates. One of the most sensitive general detection methods is sulphuric acid charring but others include spraying with water or immersion in sublimised iodine vapours. Another general detection method is to use silica plates containing a background fluorophore. After development, the plates are placed under UV light and the whole plate will fluoresce except where separated spots occur. Background fluorescence, water or iodine vapours are all less sensitive than sulphuric acid charring, but have the advantage of not altering the chemical composition of the lipids.

2.1.5 Ganglioside lipid antigens in the Guillain-Barré syndrome

Gangliosides are membrane glycolipids that are very abundant in the nervous system. They consist of two main parts: a ceramide tail that is inserted in the lipid membrane and a highly variable oligosaccharide part that protrudes externally. Sialic acid (N-acetyl neuraminic acid) has to be present for the glycolipid to be defined as a ganglioside but certain asialo-gangliosides have also been defined. Their nomenclature has been outlined by Svennerholm *et al.* (1994) and is based on the type of hexoses in the backbone, the number of sialic acids, TLC migration and isomer forms. Gangliosides are involved directly or indirectly in a range of functions including cell-growth, differentiation and recognition. They may play a role in signal transduction and can also act as receptors for bacterial toxins (Kurzchalia & Parton, 1999). The main glycolipids of importance in immune-mediated neuropathies are diagrammed in Figure 2.8.

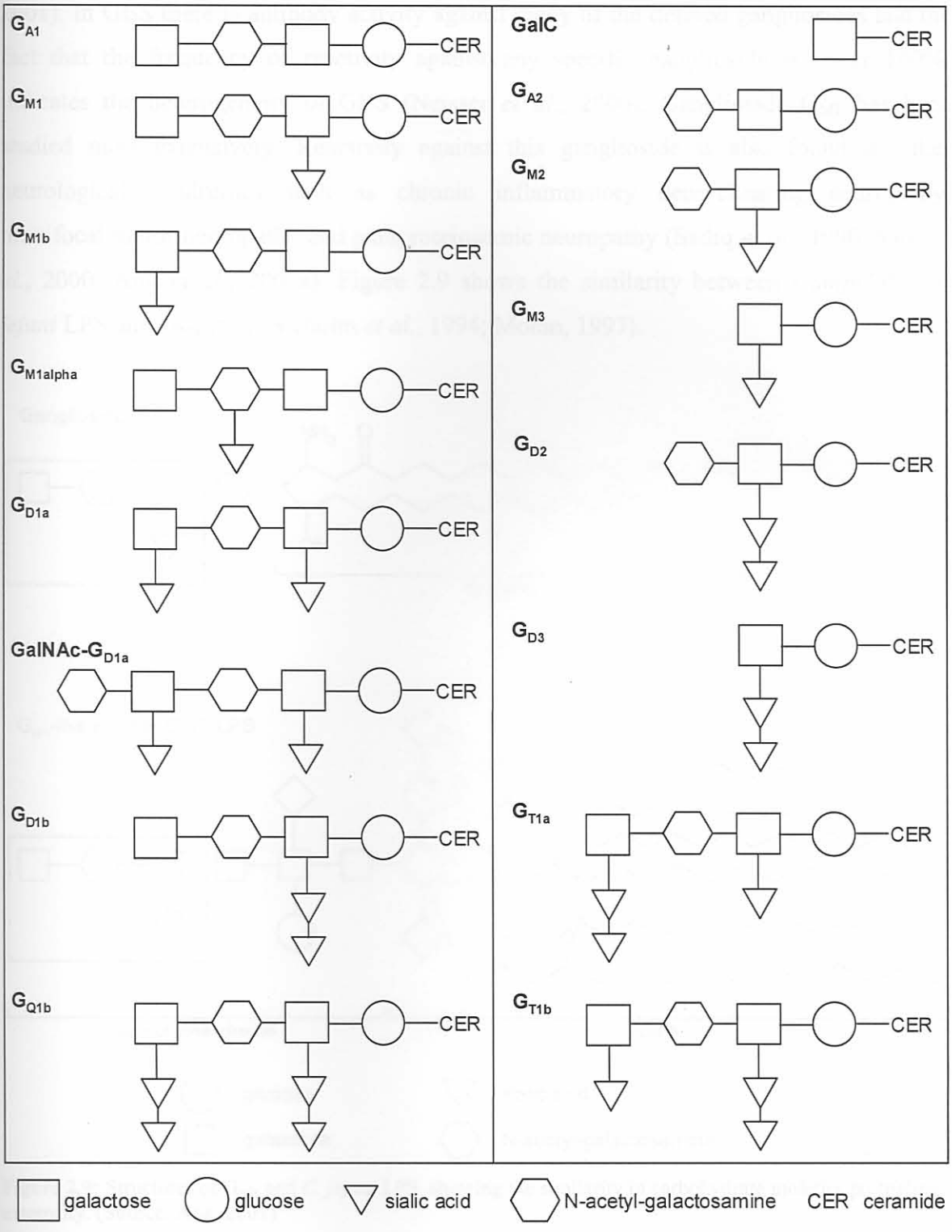

Figure 2.8: Structures of gangliosides and other glycolipids significant in GBS and other immune-mediated neuropathies. G: ganglioside, C: ceramide, Gal: galactose, GalNAc: N-acetyl-galactosamine. (Source: Ang, 2001)

Ganglioside composition differs not only between motor and sensory nerves but also between the axons and myelin of nerves. In axons, G_{M1} and G_{D1a} are the major glycolipids, and L_{M1}, G_{M3} and G_{D1b} predominates in myelin (Willison *et al.*, 1997; Aoyama *et al.*,

2001). In GBS there is antibody activity against many of the defined gangliosides and the fact that the frequency of reactivity against any specific ganglioside is never 100%, indicates the heterogeneity of GBS (Neisser *et al.*, 2000). Ganglioside G_{M1} has been studied most extensively. Reactivity against this ganglioside is also found in other neurological syndromes such as chronic inflammatory demyelinating neuropathy, multifocal motor neoropathy and paraproteinaemic neuropathy (Sadiq *et al.*, 1990, Yuki *et al.*, 2000; Ang *et al.*, 2001a). Figure 2.9 shows the similarity between *Campylobacter jejuni* LPS and G_{M1} (Svennerholm *et al.*, 1994; Moran, 1997).

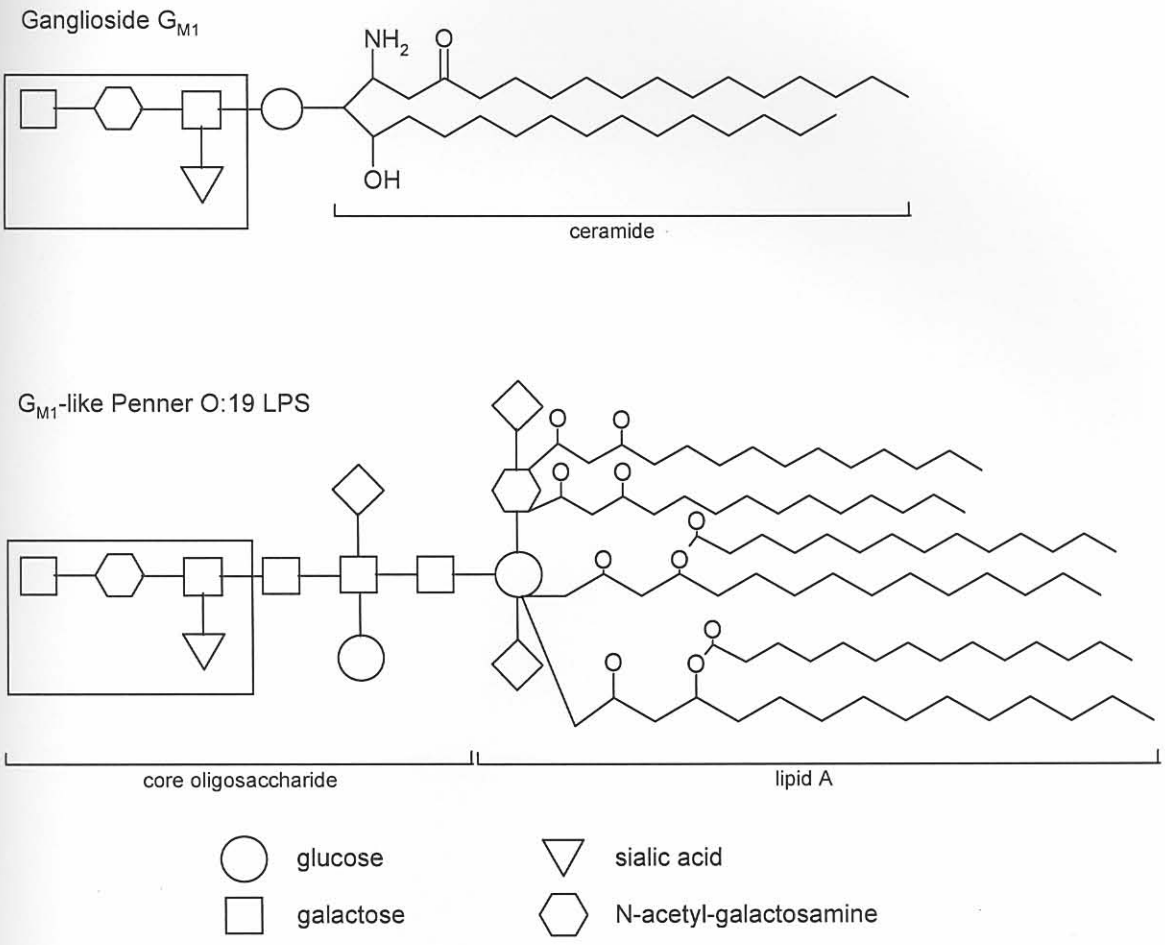

Figure 2.9: Structures of G_{M1} and *C. jejuni* LPS, showing the similarity in carbohydrate moieties protruding externally. (Source: Ang, 2001)

It has already been suggested that the onset of GBS is caused by a disturbance in the idiotype network of antibodies (Lundkvist *et al.*, 1993), triggered by the molecular mimicry between *C. jejuni* LPS and gangliosides (Ang, 2001). The biosensor method described here may be useful in supporting this hypothesis and also to quantify opposing antibody levels. Cholera toxin (CTx), a specific ligand for G_{M1} (Cuatrecasas, 1973), could

be useful as a reference for specific G_{M1} binding when determining kinetic parameters of the anti-G_{M1}, or cross-reactive GBS patient sera.

2.2 Aims

- Developing a thin layer chromatographic (TLC) system to separate mycolic acids into their subclasses
- Separation of mycolic acids (MA) on the developed TLC system
- Optimisation of a method for the immobilisation of mycolic acid-liposomes on a non-derivatised cuvette surface
- Optimisation of a method for the immobilisation of ganglioside-liposomes on a non-derivatised cuvette surface

2.3 Materials and Methods

2.3.1 Materials

Cholesterol, monosialoganglioside G_{M1} from bovine brain, L-α-phosphatidylcholine (PC) from lecithin and commercial MA from *Mycobacterium tuberculosis* were from Sigma. Sodium chloride (NaCl), anhydrous disodium hydrogen phosphate, potassium dihydrogen phosphate, iodine, general-purpose acetone and 3Å molecular sieve were supplied by Merck and analytical grade petroleum ether by Merck NT laboratories. The TLC plates (20 × 20cm with 20 × 2.5cm concentrating zone, glass support), and preparative thin layer chromato-graphy (PLC) plates (20 × 20cm with 20 × 4cm concentrating zone, glass support or 20 × 20cm without concentrating zone, glass support) were also from Merck. Analytical quality tris (hydroxymethyl) amino methane (Tris), ethylene diamine tetra-acetic acid (EDTA), chemically pure chloroform, *n*-hexane, diethyl ether, methanol, ethyl acetate and analytical grade sulphuric acid, hydrochloric acid (HCl), acetic acid, potassium bicarbonate ($KHCO_3$) and potassium hydroxide (KOH) were all from Saarchem and general purpose sodium azide (NaN_3) and sodium hydroxide (NaOH), as well as analytical grade benzene, ethanol and dichloromethane from BDH. Cetyl pyridinium chloride (CPC), saponin, guanidine thiocyanate (GSCN) and silver nitrate ($AgNO_3$) were from Sigma. For high-pressure liquid chromatography (HPLC) analyses, HPLC grade methanol and dichloromethane (BDH) were used. The C-100 internal standard was obtained from Ribi Immunochem Research Company (Hamilton, Montana, U.S.A.) and *p*-bromophenacyl-bromide (0.005mmol/ml crown ether in acetonitrile) from Pierce (Rockford, Illinois, U.S.A.). (Trimethylsilyl)-diazomethane (TMDM) was from Fluka. Double-distilled deionised water was used for all analytical experiments. Saarchem, BDH and Merck products (Darmstadt, Germany) were supplied by Merck NT Laboratories, Midrand, South Africa. Sigma and Fluka products were supplied by Sigma-Aldrich Corp., St. Louis, Missouri, U.S.A.

2.3.2 Calculations

Due to the heterogeneity of the crude self-prepared MA extract, relative MA concentrations are indicated as mass ratios. To determine molar ratios for use in G_{M1}-liposomes, it was assumed that PC contained two palmitoyl fatty acid chains and G_{M1} contained a 1:1 ratio of nervonoyl and stearoyl ceramides.

2.3.3 Analytical thin layer chromatography

Silica gel plates, with either glass or aluminium as support, were dried for two hours at 110°C and allowed to cool in a dessicator before use. Samples to be analysed were dissolved in chloroform and spotted onto the plates with a micropipette in volumes not exceeding 5µl at a time. Between 50 and 500µg of a test sample was spotted. To evaporate residual chloroform from the test samples, the plates were dried again briefly at 80°C. Mobile phases consisting of various ratios (v/v) of *n*-hexane and diethyl ether were prepared and dried overnight at 4°C with 3Å molecular sieves. Mobile phases containing ethyl acetate, petroleum ether, methanol, dichloromethane and/or acetic acid were treated similarly.

The developing tank was equilibrated with the mobile phase for at least 30 minutes prior to each experiment using paper towelling attached to the side of the tank so that the bottom just touched the mobile phase. During the experiment the mobile phase was kept dry with 3Å molecular sieve. The prepared TLC plates were lowered into the tank, the top of the tank sealed, and development allowed to take place until the eluent front reached 1-3cm from the top of the TLC plate. The plate was then removed, dried briefly at 80°C and the spots visualised.

Iodine vapours were used at first for visualisation. Iodine crystals were placed in a sealed tank at 80°C until the vapour/solid states reached equilibrium. The developed plates were placed in the tank until the spots were visible, removed and scanned using a Hewlett Packard 3200C flatbed scanner (Palo Alto, California, U.S.A.) and accompanying software. Iodine visualisation was later discontinued and replaced by sulphuric acid charring. A 65% (v/v) aqueous sulphuric acid solution was sprayed evenly onto the developed plate using an aerosol propellant (Sigma-Aldrich Corp., St. Louis, Missouri, U.S.A.). The plates were then placed at 110°C until visible spots appeared. Scanning of the plates was done as before.

2.3.4 Two-dimensional thin layer chromatography

For two-dimensional TLC, the plates were developed in the first mobile phase, dried for ten minutes at 80°C, turned through 90°, and developed in the second mobile phase. Visualisation was done with sulphuric acid charring.

2.3.5 Preparative thin layer chromatography

Preparative TLCs were either developed on plates with a 2mm or 5mm thick silica coat. The thinner plates had a concentrating zone of 2.5cm. Samples were striped at the bottom of the plates to a maximum of 10mg, dried and developed as for the analytical plates. After development, approximately 2cm of each side of the plate was removed so that a small amount of the developed sample was on each strip. The strips were visualised by sulphuric acid charring, compared to the rest of the plate and the bands identified accordingly. The silica containing the identified bands were scraped off the plate, powdered in a conical flask and extracted with chloroform using a vacuum filtration system and Whatman number 1 filter papers. The silica was washed thoroughly (five times) with chloroform to ensure a high yield. Samples were dried at 85°C under a steady stream of nitrogen gas, dissolved in small volumes of chloroform, transferred to amber vials and dried again under nitrogen gas for use in HPLC or HPLC-MS analysis.

Yuan *et al.* (1997) described the preparative separation of MA. This was attempted analytically by using dried analytical TLC plates as described (*see* par 3.4.2). After spotting the different MA samples, the plate was developed five times consecutively with 19:1 *n*-hexane:ethyl acetate (v/v), with drying at 80°C for five minutes in-between every development. Visualisation was done by sulphuric acid charring.

2.3.6 Complex argentation thin layer chromatography

A complex two-dimensional argentation TLC done by George *et al.* (1995) was attempted. An analytical TLC plate was submerged in a 10% (w/v) aqueous $AgNO_3$ solution so that 16cm of the plate was impregnated with $AgNO_3$ and a strip free of $AgNO_3$ would be left at one side. The plate was dried for an hour at room temperature and thereafter activated at 50°C, 80°C and 110°C for 20, 20 and 40 minutes respectively. The plate was allowed to cool in a dessicator, re-activated for 30 minutes at 110°C and used immediately. After MA was spotted on a corner outside the $AgNO_3$, the plate was developed twice into the strip without $AgNO_3$ with 19:1 (v/v) *n*-hexane:ethyl acetate. Thereafter, the plate was turned through 90° and developed three times into the $AgNO_3$ impregnated part with 17:3 (v/v) petroleum ether:diethyl ether. Between developments, the plate was dried for five minutes at 80°C. Both mobile phases were dried with 3Å molecular sieve overnight. Visualisation was done by sulphuric acid charring.

2.3.7 Preparation of *Mycobacterium tuberculosis* mycolic acids

Mycobacterium tuberculosis H37Rv, a virulent strain originally isolated from an infected human lung, was used for isolation of MA. The lyophilised culture was purchased from the American Type Culture Collection (ATCC 27294), Maryland, U.S.A. The bacteria were cultured, harvested, saponified and crudely extracted as described elsewhere (Goodrum *et al.*, 2001). The crude extract of MA was subjected to a preliminary purification step and then purified further on a countercurrent apparatus using a triphase solvent system comprising 42:39:19 chloroform:methanol:water (v/v) as described elsewhere (Goodrum *et al.*, 2001).

2.3.8 Preparation of *Mycobacterium avium* mycolic acids

Mycolic acids from *M. avium* were isolated similarly to that of *M. tuberculosis* but the method arrested after the addition of Reagent C (*see* par 2.3.8.1) during the crude extract preparation. Countercurrent purification was not performed on *M. avium* MA. The method used by Kaneda *et al.* (1986) was then applied as follows:

Crystalline, crude *M. avium* MA (after Reagent C) was dissolved in the two phases of a 42:39:19 (v/v) chloroform:methanol:water mixture. Two hundred millilitres of the bottom phase was added to the MA, the mixture shaken well, and 200ml upper phase added. After agitation, the bottom chloroformic phase was removed and extracted again with 200ml aqueous upper phase. The chloroformic phase was evaporated in a Buchi Roto-evaporator RE 120. Twenty millilitres of a 10:20:1 (v/v) benzene:methanol:sulphuric acid mixture was added to the MA and shaken vigorously. To this, 10ml *n*-hexane was added. The *n*-hexane partitioned mainly to the top benzenic layer. The bottom layer was removed, re-extracted with 10ml *n*-hexane, and the two *n*-hexane fractions combined. The hexanic fraction was extracted with 20ml water and evaporated on a Buchi evaporator. The concentrated MA in the flask after evaporation was dissolved in chloroform, evaporated again, washed with methanol, evaporated again and dissolved a second time in chloroform and evaporated as above to remove traces of benzene. The dry MA was finally dissolved in a small volume of chloroform, transferred to an amber vial and evaporated at 85°C under a steady stream of nitrogen gas.

2.3.9 High pressure liquid chromatography

2.3.9.1 Reagents

A: 25% (w/v) KOH in 1:1 (v/v) water:methanol

B: 1:1 (v/v) HCl:water

C: 2% (w/v) $KHCO_3$ in 1:1 water:methanol

D *p*-bromophenacylbromide in Crown ether

E: 1:1 (v/v) Reagent B:methanol

High molecular weight (C-100) internal standard

2.3.9.2 Derivatisation of mycolic acids

When the sample (eluted from TLC) was still in chloroform, it was added to a vial containing an aliquoted amount of internal standard (5µg). To derivatise the MA, 1.9ml Reagent A was added to each sample and heated to 85°C for 15 minutes in a heat block. Samples were allowed to cool to room temperature before adding 1.5ml Reagent B. Five hundred microlitres chloroform was added to each sample, vortexed for 30 seconds and the chloroformic (lower) phase removed with a glass Pasteur pipette and transferred to a clean vial. The chloroform extraction step was repeated once more and then the combined chloroformic extracts were evaporated under a steady stream of nitrogen gas to dryness at 85°C in a heat block. One hundred microlitres Reagent C was added and again evaporated to dryness as before. The samples were allowed to cool to room temperature and 1ml chloroform was added. One hundred microlitres Reagent D was added, vortexed for 30 seconds and incubated at 85°C in a heat block for 20 minutes. Samples were allowed to cool to room temperature, 1ml Reagent E added, vortexed for 30 seconds and the phases allowed to separate. The chloroform (lower) phase was transferred to a clean vial as before and dried under a steady stream of nitrogen gas at 85°C in a heat block.

2.3.9.3 Reverse phase HPLC

Samples were dissolved in 220µl dichloromethane, vortexed at 100% for 30 seconds and filtered through 0.22µm Teflon filters into pre-prepared inserts placed in 1.8ml vials. The vials were loaded in an AS-2000 autosampler (Hitachi Ltd., Tokyo, Japan)and 15µl volume of each sample was injected. The HPLC system was fitted with a Waters prefilter and a Luna 5µm C18 column (4.6mm x 250mm) obtained from Phenomenex (Torrance, California, U.S.A.) packed with 5µm spherical particles with a pore size of 10nm. An L-

6200A pump (Hitachi Ltd., Tokyo, Japan) was used to generate a flow rate of 1ml/min and the column was equilibrated with 98:2 (v/v) methanol:dichloromethane before use. The solvents were HPLC grade methanol and dichloromethane, run at the following methanol gradient (time indicated in minutes):

t = 0	100%
t = 2	98%
t = 15	55%
t = 25	35%
t = 30	35%
t = 35	98%
t = 50	98%

Detection was done at 260nm with an L-4500 UV detector (Hitachi Ltd., Tokyo, Japan). Peaks were quantified by area and those smaller than 30 000 units rejected. Mycolic acid yield was calculated as a ratio of the mycolic acid peak area and the internal standard peak area:

$$MA\ (\mu g) = \frac{MA\ peak\ area \times 5\mu g}{Internal\ std\ peak\ area} \qquad (2.1)$$

2.3.10 Methylation of mycolic acids

(Trimethylsilyl)diazomethane (TMDM) was purchased as a 2M solution in *n*-hexane. The solution was aliquoted in 1ml volumes and one aliquot was dried under a stream of nitrogen at 85°C and redissolved in 1ml diethyl ether. Twenty microlitres of the MA samples (10mg/ml for commercial and self-prepared *M. tuberculosis* MA and undetermined concentration for *M. avium* MA) were incubated with 5µl of either diethyl ether- or *n*-hexane-dissolved 2M TMDM at room temperature for one hour.

2.3.11 Thin layer chromatography of methylated mycolic acids

The total volume of the TMDM incubated samples was loaded onto a silica plate that had been dried for two hours at 110°C. After loading, the plate was dried briefly at 80°C and then developed five times consecutively in a mobile phase containing 9:1 (v/v) petroleum

ether:diethyl ether. Between developments, the plate was dried at 80°C for ten minutes. Visualisation was done by sulphuric acid charring.

For the determination of the number of developments necessary to resolve the MA subgroups, a new sample was spotted next to the previous spot onto the plate after each development so that five spots subjected to different numbers of development could be observed.

For the preparative TLC of the methylated MA, a total of 10mg (ten times 10µl of a 100mg/ml chloroform solution) self-prepared *M. tuberculosis* MA that had been methylated (*see* par 2.3.10) was striped on a preparative TLC plate. The plate was developed as described, the sides removed and visualised by sulphuric acid charring before compared with the remainder of the plate to identify the spots to be eluted.

2.3.12 Electron-impact mass spectrometry

Samples dissolved in chloroform were subjected to gas chromatography mass spectrometry (GC-MS) using a Varian 3400 gas chromatograph equipped with a Finnigan TSQ-700 triple quadrupole mass spectrometer (San Jose, California, USA), a Waters 600-MS system controller, Waters 490-MS programmable multi-wavelength detector (Milford, Massachusetts, USA) and a split/splitless injection port. The ZB624 column used was 30m long and had an internal diameter of 0.25mm with a 1.4µm thick film coating. The carrier gas was helium at a backpressure of 14psi. The injection port and transfer line temperatures were both set at 250°C while the split vent flow was set at 60-70ml per minute and the septum purge at 3-5ml per minute. Samples were dissolved in a 1:4 isopropyl alcohol:acetonitrile solution saturated with ammonium acetate as proton source and 1µl volumes were injected. The oven temperature was started at 40°C, ramped to 240°C with 10°C per minute increments and held for 15 minutes. The ionisation mode was electron impact (70eV) with the ion source temperature set at 200°C. The filament current was 200µA, the electron multiplier voltage 1kV and the lens voltage –10V.

2.3.13 Biosensors

Three different IAsys biosensors were used at the following localities:

1. Department of Immunology, Erasmus University Rotterdam, Rotterdam, Netherlands
2. R&D department, IAsys Affinity Sensors, Cambridge, U.K.
3. Department of Biochemistry, University of Pretoria, Pretoria, South Africa

Non-derivatised cuvettes were supplied by the biosensor manufacturer, IAsys Affinity Sensors, Cambridge, U.K.

2.3.14 Mycolic acid-liposome preparation

Mycolic acids were dissolved in chloroform and 100µg quantities aliquoted into amber vials and stored at 4°C. Phosphatidylcholine and cholesterol stock solutions were freshly prepared in chloroform at concentrations of 10mg/ml. Sixty microlitres PC and 30µl cholesterol were added to vials containing 0.1mg MA. The vials were dried in a heat block at 85°C under a steady stream of nitrogen gas. These vials were stored at 4°C until the day of use. Two millilitres phosphate buffered saline (PBS) with 0.025% (w/v) sodium azide and 1mM EDTA (PBS/AE), were added to a vial containing the dried lipids, the lipids melted at 85°C in a heat block for ten minutes, vortexed at 100% for one minute and then sonified in a Branson sonifier with a microtip set at a pulsed energy transfer at 20 duty cycles, output level 2, for 20 strokes or one minute. The melting step is crucial as MAs are waxes with higher melting points than PC and cholesterol and do not solvate easily. This was followed by another minute of vortexing at 100%. This resulted in a 0.5mg/ml liposome suspension containing PC, cholesterol and MA in a 6:3:1 mass ratio respectively.

2.3.15 Mycolic acid-liposome immobilisation on biosensor cuvettes

Cuvettes were washed with PBS/AE until a stable baseline could be maintained for at least five minutes. The cells were aspirated and 50µl of a 20µg/ml CPC in PBS/AE solution was added. After ten minutes the cells were washed five times with 60µl PBS/AE, then 25µl PBS/AE was added until a stable baseline was achieved. Twenty-five microlitres of the desired liposome solution was added and the response monitored for ten minutes. Cells were then washed five times with 60µl PBS/AE and immediately after that, treated five times with 60µl 1mg/ml saponin in PBS/AE. The cells were incubated with saponin for at

least ten minutes and until a stable baseline was achieved before a final five times wash with 60µl PBS/AE. Interaction analysis could be continued from this point.

Due to a response difference among saponin batches, it was necessary to titrate the amount of saponin required each time a new batch of saponin was used.

2.3.16 Mycolic acid-liposome cuvette regeneration

Unlike other surfaces where proteins and other molecules are immobilised covalently, regeneration of liposome coats on a non-derivatised surface partly removes the liposome coat. Subsequent liposome immobilisations or interaction analyses cannot be carried out on this partial coat. Accordingly, it is important that everything be stripped from the cell surface during a regeneration step and that a new liposome coat is prepared for a subsequent interaction analysis. Regeneration was initially performed with several steps including 95% ethanol to remove all fatty deposits and 3.5M GSCN to regain sharp resonance scan peaks. This was later changed to a three times wash step with 60µl 12.5M KOH, and later optimised to three times 50µl 95% ethanol for 30 seconds, followed by three times 80µl PBS/AE for one minute and five times 60µl PBS/AE. Following this was a five times wash step with 60µl 12.5M KOH for two minutes and again three times 80µl PBS/AE for one minute and five times 60µl PBS/AE. The buffer wash steps were included to ensure that both the ethanol and KOH are washed away thoroughly as both would severely affect liposome immobilisation. After the last PBS/AE step, the cuvette would be ready for another round of CPC activation, liposome immobilisation and interaction analysis.

2.3.17 Ganglioside-liposome preparation

Ganglioside G_{M1} was dissolved in chloroform and 100µg quantities aliquoted into amber vials and stored at 4°C. Phosphatidylcholine and cholesterol stock solutions were freshly made in chloroform at concentrations of 1mg/ml. Varying quantities of PC and cholesterol were added to the vials containing 100µg G_{M1} to make either mass or molar ratios of the different lipids as desired. For optimised G_{M1}-liposomes, 878µl PC was added to one vial containing 100µg G_{M1}. PBS/AE or a Tris based buffer (50mM Tris, 200mM NaCl, 3mM NaN_3, 1mM Na_2EDTA) was added to a liposome concentration of 0.5mg/ml, the solution

vortexed for one minute at 100%, sonified as above, and vortexed again for one minute at 100%. The G_{M1}-liposomes did not need to be melted since they did not contain MA.

2.3.18 Ganglioside-liposome immobilisation on biosensor cuvettes

After using the same method for MA-liposome immobilisation initially, the method was optimised as described elsewhere (*see* 2.5 Results). Fifty microlitres G_{M1}-liposomes were added directly to aspirated cells containing residual 20mM HCl (~15µl) after regeneration. After incubating the liposomes for ten minutes, the cells were washed four times with 60µl PBS/AE or Tris buffer, four times with 60µl 10mM NaOH and five times with 60µl PBS/AE or Tris buffer. Thereafter the cells were aspirated and 25µl of PBS/AE or Tris buffer was added and a stable baseline was obtained for at least five minutes before interaction analyses could proceed.

2.3.19 Ganglioside-liposome cuvette regeneration

The same regeneration protocol as for MA-liposomes was used initially but changed later to a modified method of Altin *et al.* (2001). After dissociation events, cells were washed four times with 60µl absolute ethanol, seven times with 100µl water, five times with 60µl 12.5M KOH and incubated at this step for two minutes. The cells were washed again seven times with 100µl water and then three times with 2M HCl and four times with 20mM HCl. After the 20mM HCl step, a stable baseline would be obtained for at least five minutes before the cells could be aspirated and liposomes added directly for the next round of immobilisation and interaction analysis.

2.4 Results

2.4.1 Separation of the mycolic acid subclasses with thin layer chromatography

2.4.1.1 Optimisation of detection method

Appropriate detection techniques for lipids or waxes include the use of iodine vapours, sulphuric acid charring and water vapour. Iodine vapour provides a general non-specific detection method and can be used to identify almost any lipid (Skipski & Barclay, 1969). Sulphuric acid oxidises all biological material to carbon dioxide and water as well as elemental carbon, which remains visible on TLC plates. Water vapour is adsorbed by the hygroscopic silica plates used, except where it is covered by a lipid spot or smear, thereby visualising the lipid. Although the water vapour technique is non-invasive and ideal for preparative purposes, it is limited in sensitivity. Iodine vapour is more sensitive and also non-invasive (iodine vapours sublimate after a while) but compared to sulphuric acid charring it is less sensitive (Figure 2.10). Throughout the TLC experiments, cholesterol was spotted as a control lipid because of its active mobility in diverse eluents. Also, to enable compensation for the effects of possible irregular eluent fronts, cholesterol samples were spotted on either side of the plates and/or in between test samples.

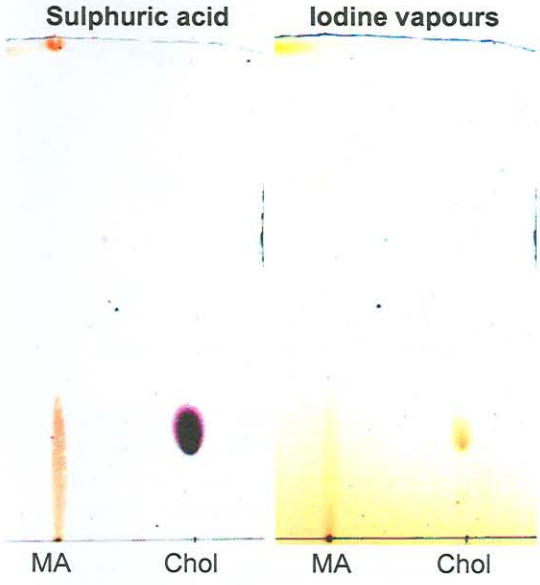

Figure 2.10: A comparison between the sensitivities of sulphuric acid charring and iodine vapours as visualisation techniques for MA and cholesterol on a silica TLC plate. The plates were developed with 50:50 diethyl ether:*n*-hexane as eluent. MA - *M. tuberculosis* mycolic acids, Chol - cholesterol

2.4.1.2 Thin layer chromatographic comparison of different mycolic acid sources

It has been reported that MA from *M. avium* separate into three distinct species (α-, keto- and methoxy-MA) on TLC (Kaneda *et al.*, 1986) using 20:80 diethyl ether:*n*-hexane. Using a crude extract of *M. avium* MA as a positive control as well as commercially available *M. tuberculosis* MA, a TLC was run with 20:80 diethyl ether:*n*-hexane (Figure 2.11). Pure commercial *M. tuberculosis* MA was used to compare it with the purity of the crude *M. avium* and self-prepared *M. tuberculosis* MA samples. Neither the commercial nor the self-prepared *M. tuberculosis* MA moved much from the origin. Most of the MA of *M. avium* remained behind at the origin but three faint spots with R_f values of 0.28, 0.51 and 0.67 were obtained. Because little mobility was observed with the *M. tuberculosis* MA, it was expected that these spots represent non-MA components present in the crude *M. avium* MA extract.

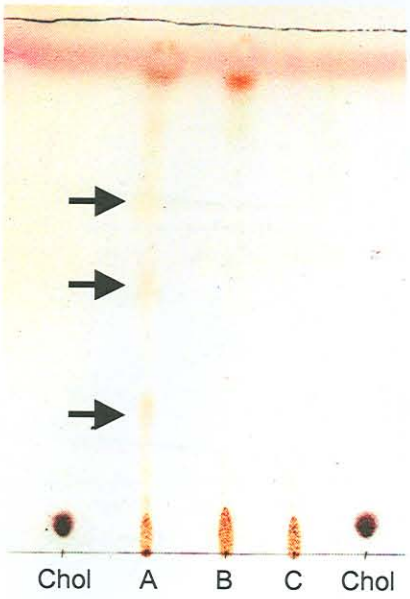

Figure 2.11: A thin layer chromatogram of *M. avium*, *M. tuberculosis* and commercial MA from *M. tuberculosis*, developed with 20:80 diethyl ether:*n*-hexane and visualised by sulphuric acid charring. Chol - cholesterol, A - *M. avium* MA, B - *M. tuberculosis* MA, C - commercial *M. tuberculosis* MA.

All the MA samples except the commercial MA showed a distinct spot at the very front of the mobile phase. It is not certain what this spot represents, but it may be a contaminant present in the solvents used for MA extraction. The next step was to analyse the different

fractions of *M. avium* as well as *M. tuberculosis* to confirm the localisation of the MA on the TLC chromatogram.

2.4.1.3 *High pressure liquid chromatography identification of mycolic acids in thin layer chromatography-separated samples*

Preparative TLCs were run separately on MA from both *M. avium* and *M. tuberculosis* using the same eluent as before, i.e. 20:80 diethyl ether:*n*-hexane. After the plates were developed, the sides were removed, visualised with sulphuric acid charring, compared with the remainder of the plate, and the strips of silica removed and eluted accordingly. The eluted samples were analysed by HPLC according to Goodrum *et al.* (2001). Figure 2.12 shows the TLC chromatogram as well as the HPLC analyses of pure MA from *M. tuberculosis* and the bands eluted from the TLC plate.

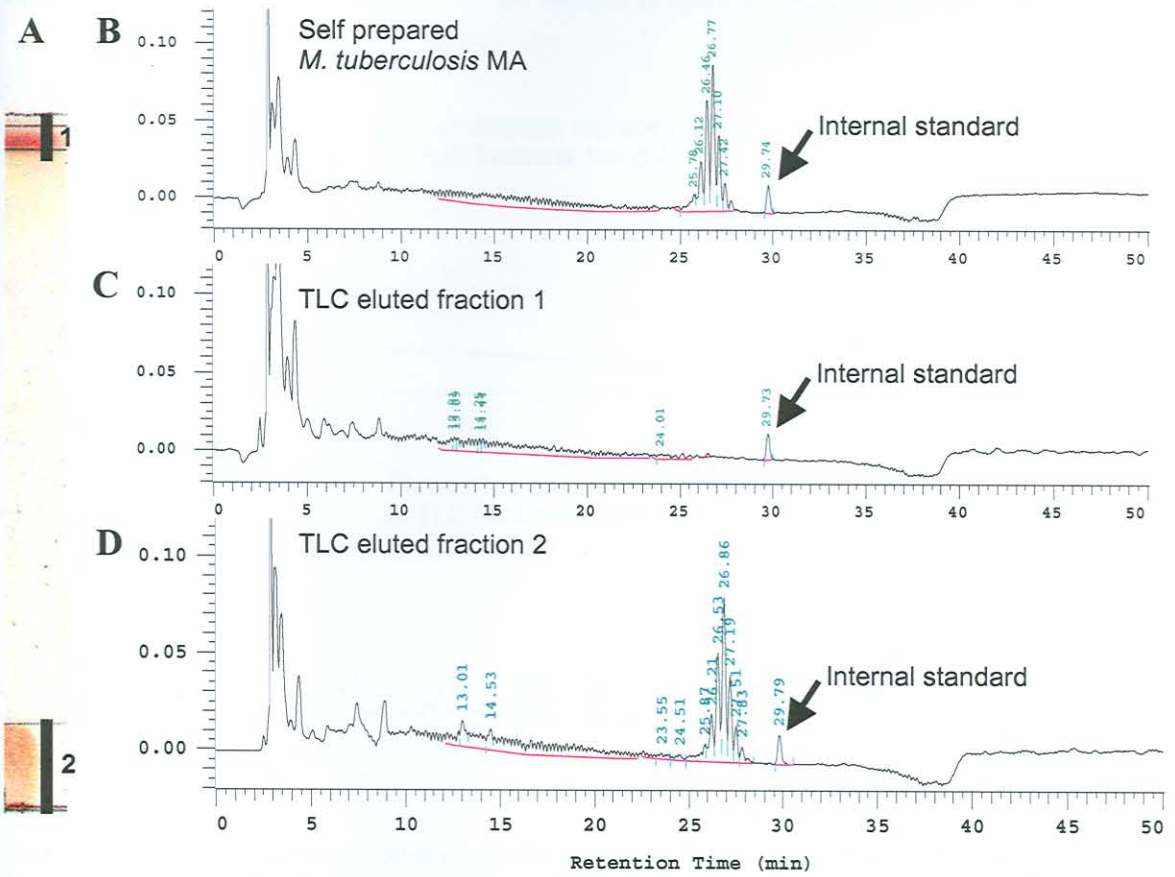

Figure 2.12: High-pressure liquid chromatography analysis of *M. tuberculosis* TLC bands. **(A)** The preparative TLC plate showing the bands isolated and extracted for analysis. **(B)** The HPLC chromatogram of an unseparated MA sample showing the typical retention time of the peak cluster of MA at a retention time of 26 minutes as well as the internal standard at a retention time of 30 minutes (indicated by arrows). **(C)** The HPLC chromatogram of the top eluted fraction of the TLC plate indicating the absence of MAs. **(D)** The HPLC chromatogram of the bottom eluted fraction of the TLC plate, confirming the presence of MA in the typical region of 25-8 minutes.

The cluster of nine peaks around a retention time of 26.8 minutes is characteristic of MA (Figure 2.12B). The nine peaks are due to the different chain lengths of MA species found. It is known that every peak representing a chain length contains all three subgroups (α-, keto- and methoxy-) in the same relative ratio. The second HPLC chromatogram shows that there are indeed no MA to be found in the band at the front of the TLC chromatogram (Figure 2.12C) and that all the *M. tuberculosis* MA remained at the origin (third HPLC chromatogram, Figure 2.12D).

Similarly, the HPLC analysis of the *M. avium* bands from the preparative TLC showed that the band at the elution front (Fraction 1) did not contain any MA (Figure 2.13B). Mycolic acids were found at the origin (Fraction 4) and the smear directly above (Fraction 3), similar to what was found with the *M. tuberculosis* sample, albeit at a much lower concentration due to the crudeness of the sample (Figure 2.13C).

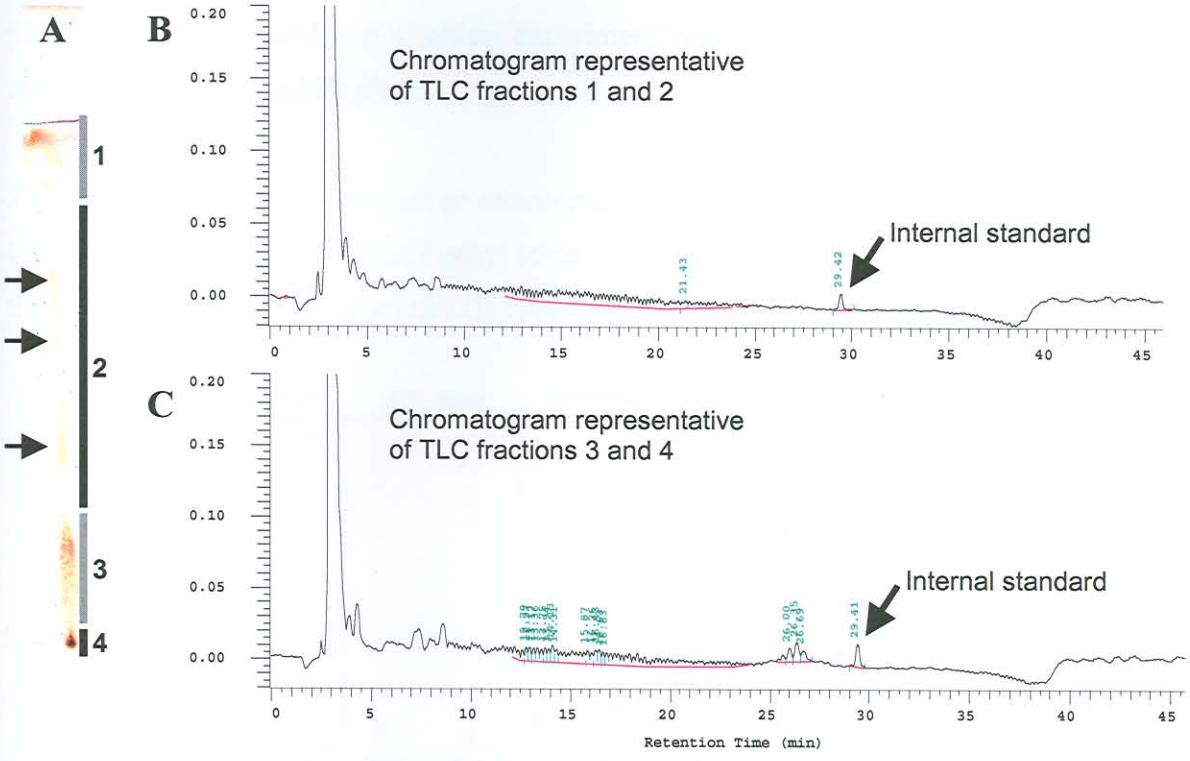

Figure 2.13: High-pressure liquid chromatography analysis of *M. avium* TLC bands. **(A)** The preparative TLC plate showing the bands isolated and extracted for analysis. Arrows indicate possible separated bands. **(B)** A representative HPLC chromatogram of eluted fractions 1 and 2 of the TLC plate indicating the lack of MAs. **(C)** A representative HPLC chromatogram of eluted fractions 3 and 4 of the TLC plate confirming the presence of MA in the typical region of 25-8 minutes.

The three spots that separated in the middle (indicated by arrows in Figure 2.13A) were pooled together for HPLC analysis (Fraction 2), and were shown not to contain any MA at

all (Figure 2.13B). This confirmed that the three faint separated spots of *M. avium* were not separate MA subgroups.

A curious observation was that in all the TLC experiments done, even though the experiments were faithfully followed as described in the literature, most of the MA remained largely immobile at the origin. This was in contrast to Kaneda *et al.* (1986) in which all the MA species had R_f values of at least 0.43 on similar TLC plates developed in this eluent. Comparing the initial experiments where the mobile phase contained 6:100 diethyl ether:*n*-hexane with later experiments where a ratio of 20:80 was used, it was noticed that the mobility of the MA correlate positively with the increase in diethyl ether concentration of the mobile phase. This trend was also noticed in the cholesterol samples that were spotted onto all plates as a control. The deduction that an increase in diethyl ether concentration would enhance MAs mobility seemed logical, since MA was found to be completely soluble in diethyl ether but much less so in *n*-hexane (personal communication, Mrs. S. van Wyngaardt). A titration experiment was set up to determine the optimum composition of the mobile phase.

2.4.1.4 Titration of diethyl ether concentration in the mobile phase

Increasing the concentration of diethyl ether in the mobile phase increased the R_f values of the cholesterol and the MA smears (Figure 2.14).

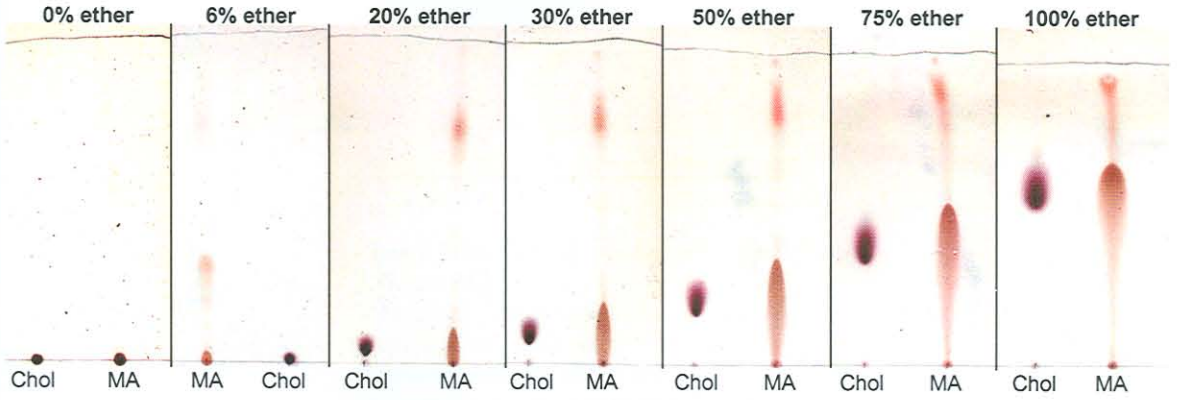

Figure 2.14: The effect of diethyl ether concentration in *n*-hexane as the eluent on the mobility of cholesterol and *M. tuberculosis* MA on TLC plates. Visualisation was done by sulphuric acid charring.

The much higher R_f values obtained with TLC using the high diethyl ether concentrations, suggested that a mistake was made in the article by Kaneda *et al.* (1986). It is much more likely that they have used 80:20 diethyl ether:*n*-hexane instead of 20:80. The R_f value of

0.51 obtained for MA with the 75% diethyl ether concentration, correlates well with the average R_f value of 0.52 obtained for the unresolved spot in the article by Kaneda *et al.* (1986) that was reportedly obtained with 20% diethyl ether in *n*-hexane. In subsequent experiments a ratio of 80:20 diethyl ether:*n*-hexane (v/v) was used instead of 20:80.

*2.4.1.5 Separation of mycolic acids with 80:20 diethyl ether:*n*-hexane*

Developing a TLC plate loaded with various MA species in 80:20 diethyl ether:*n*-hexane improved the mobility of the smears containing MA (*see* Figures 2.12 and 2.13) but did not effect any separation of the subgroups (Figure 2.15). All the MA smears had similar R_f values (0.88); much higher than those obtained with 20:80 diethyl ether:*n*-hexane (0.10). However, no distinct separate spots could be observed for the different subgroups of MA for any of the different MA species tested. No faint spots were observed above the smear for *M. avium* MA as was seen with the 20:80 diethyl ether:*n*-hexane development (*see* Figure 2.11), and it was assumed that the smear and origin both contained MA whereas the whole part above the smear did not, as indicated in Figure 2.13.

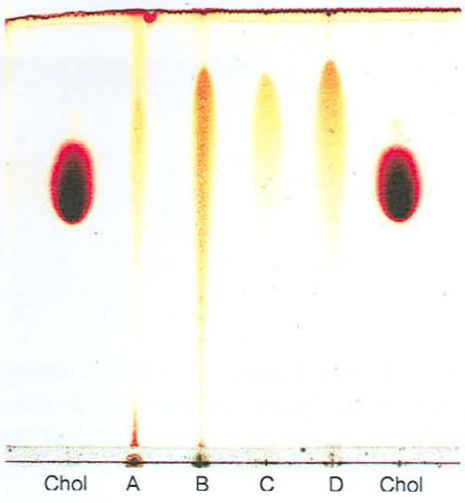

Figure 2.15: Comparing the mobilities of different MA samples on a TLC plate with 80:20 diethyl ether:*n*-hexane as mobile phase. Visualisation was done by sulphuric acid charring. Chol - cholesterol, A - *M. avium* MA, B - *M. tuberculosis* MA, C - 5µg commercial *M. tuberculosis* MA, D - 10µg commercial *M. tuberculosis* MA.

2.4.1.6 Effect of acetic acid in the mobile phase on mycolic acid mobility

It was suggested (personal communication, Dr. Chris Parkinson) that a lowering of pH of the mobile phase might facilitate the separation of the MAs. Since only a small amount of

acid could cause a pronounced drop of pH in the small volume of unbuffered mobile phase, it was necessary to use a weak acid like acetic acid and then only in small volumes. Adding a single drop of glacial acetic acid to 50ml of diethyl ether:*n*-hexane did not have any significant outcome in terms of the separation of the MA subgroups (not shown). The mobile phase composition was switched around to 20:80 diethyl ether:*n*-hexane as it was used before and a similar experiment carried out. No separation of MA could be visualised when the original eluent concentration was used (not shown).

Since such small volumes of acid and unbuffered mobile phase were involved it was possible that the amount of acetic acid could be crucial, maybe even a cause for the difference in R_f values between successive experiments. To test this, increasing amounts of acetic acid were added to 20ml of 80:20 diethyl ether:*n*-hexane. Appropriate volumes of the commercial and self prepared *M. tuberculosis* MA were spotted on separate plates and developed (Figure 2.16). No separation could be observed in any of the plates developed and it was concluded that acetic acid does not affect separation in a mobile phase of 80:20 diethyl ether:*n*-hexane.

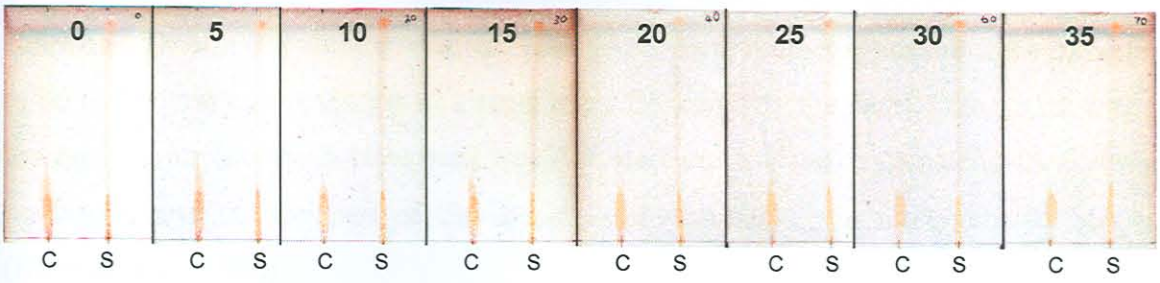

Figure 2.16: Thin layer chromatograms to titrate the optimal amount of acetic acid added to 20ml of the mobile phase (20:80 diethyl ether:*n*-hexane). Numbers indicate the volume (µl) of glacial acetic acid added. Visualisation was done by sulphuric acid charring. C - commercial *M. tuberculosis* MA, S - self-prepared *M. tuberculosis* MA.

2.4.1.7 Other methods of mycolic acid separation

According to Yuan *et al.* (1997), MA could be separated by developing a MA loaded plate five times with a 1:19 ethyl acetate:hexanes (v/v) mobile phase. The publication did not indicate the composition of the hexanes and the experiment was repeated using *n*-hexane as a substitute for hexanes. No separation could be observed for commercial- or self-prepared *M. tuberculosis* MA, and the smears observed had similar small R_f values (0.18). For *M. avium* MA very faint separated spots could be observed, similar to the spots observed with 20:80 diethyl ether:*n*-hexane developed plates. Because separated spots of

M. avium MA developed in diethyl ether:*n*-hexane did not contain MA (Figure 2.13), it was assumed that this also applied to the separated spots observed here. This method was therefore abandoned.

Another complex method described by George *et al.* (1995) was investigated. This method involves $AgNO_3$ impregnation of part of a TLC plate. The MA sample was developed twice with 19:1 hexanes:ethyl acetate into the strip not containing any $AgNO_3$ and three times into the $AgNO_3$ impregnated layer with 17:3 petroleum ether:diethyl ether. Once again the composition of the hexanes was not mentioned in the article and *n*-hexane was used as substitute in the same concentration. Sulphuric acid charring visualised a large spot with two much smaller spots at its edge, close to the origin (not shown). The MA migrated relatively little in the first dimension but not at all into $AgNO_3$ impregnated layer. This observation was contrary to what was expected and further experimentation with this method was abandoned.

2.4.1.8 Preparative isolation of mycolic acid subgroups

The separation of MA into different subgroups using TLC appeared to be quite a challenge. Drawn-out smears obtained with 80:20 diethyl ether:*n*-hexane were considered to be the closest one could get to a separation. Conceivably the part of the smear with the lowest R_f value (i.e. the bottom part) would contain more of the oxygenated MA (keto- and methoxy-) and the top part of the smear would contain the non-oxygenated MA (α-) (Kaneda *et al.*, 1986).

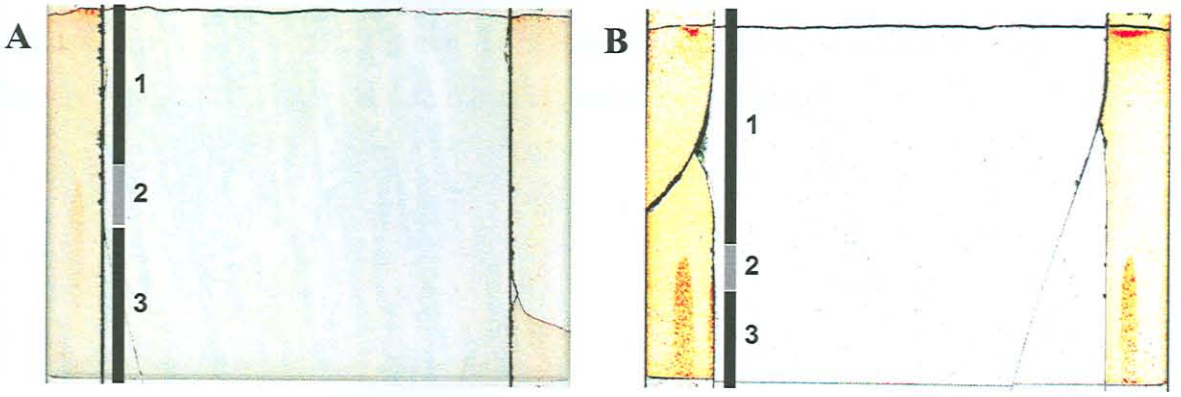

Figure 2.17: Preparative TLC plates developed with 80:20 diethyl ether:*n*-hexane and visualised by sulphuric acid charring. Fractions collected are numbered and the vertical bars indicate the extent of fraction collection. **(A)** Commercial *M. tuberculosis* MA. **(B)** Self-prepared *M. tuberculosis* MA.

To test this, commercial and self-prepared *M. tuberculosis* MA were striped on preparative TLC plates and developed in 80:20 diethyl ether:*n*-hexane. The fractions were defined as indicated (Figure 2.17), eluted and sent for electron-impact mass spectrometry (EI-MS) analysis at the Council for Scientific and Industrial Research (CSIR, Modderfontein, South Africa).

2.4.1.9 Electron-impact mass spectrometry

Electron-impact mass spectrometry done at the CSIR (Modderfontein, South Africa) showed very complex, virtually uninterpretable fragmentation patterns (Figure 2.18). However, analysis of the spectra of the different parts of the smears obtained with self-prepared *M. tuberculosis* MA (Figure 2.17B) indicated that the bottom part of the smear produced a larger number of small fragments than the top part. This may be indicative of oxygen-containing functional groups on the side chains of the MA. Such functional groups provide sites for pyrolysis and will lead to the fragmentation pattern seen. Since it is known that the oxygenated keto- and methoxy-MAs contain oxygenated functional groups, it was concluded that the bottom part of the smear does contain a higher percentage of oxygenated MA compared to the top part of the smear.

Due to the complex fragmentation patterns it was decided that the EI-MS data was inconclusive and together with the fact that the sizes of the MA were expected to be above 1000Da, it was decided that matrix-assisted laser desorption/ionisation time-of-flight mass spectrometry (MALDI-TOF MS) would be better suited to identify the different MA subclasses. Initial experimentation with MALDI-TOF MS was also inconclusive and it was suggested (personal communication: Dr. Caswell Hlongwane) to do a methylation step of the MA using TMDM even before it was loaded onto TLC plates.

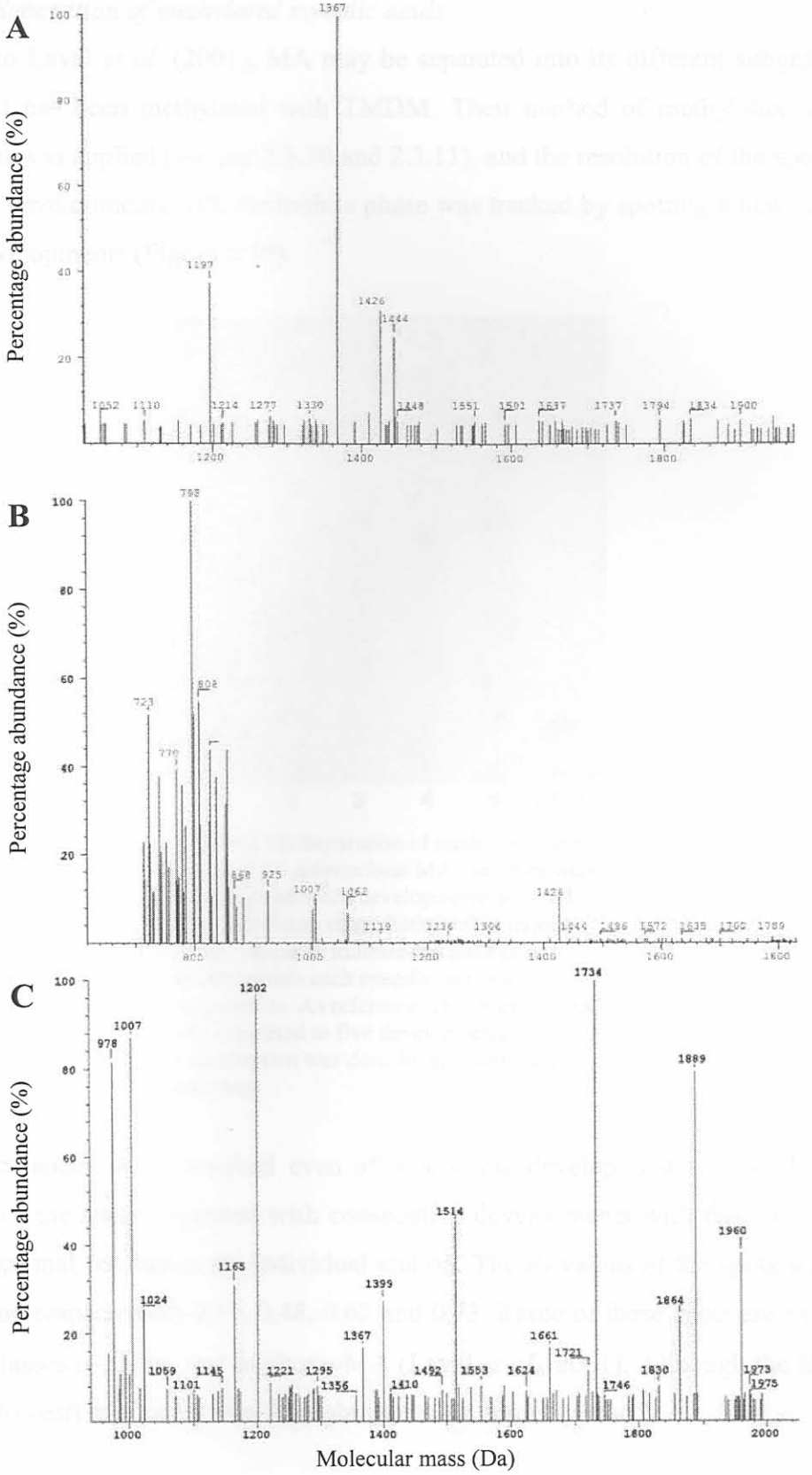

Figure 2.18: Electron-impact mass spectra of TLC separated self-prepared *M. tuberculosis* MA. **(A)** Mass spectrum of top part of the smear (Fraction 2 of Figure 2.17B). **(B)** Mass spectrum of bottom part of the smear (Fraction 3 of Figure 2.17B). **(C)** Mass spectrum of unseparated self-prepared *M. tuberculosis* MA.

2.4.1.10 Separation of methylated mycolic acids

According to Laval *et al.* (2001), MA may be separated into its different subgroups with TLC after it has been methylated with TMDM. Their method of methylation and TLC development was applied (*see* par 2.3.10 and 2.3.11), and the resolution of the spots during consecutive developments with the mobile phase was tracked by spotting a new sample in-between developments (Figure 2.19).

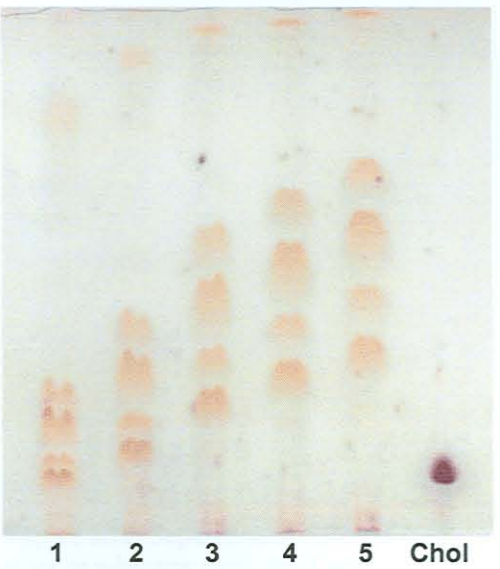

Figure 2.19: Separation of methylated self-prepared *M. tuberculosis* MA. Samples were spotted in-between developments with 9:1 (v/v) petroleum ether:diethyl ether mobile phase. Numbers indicate the number of developments each specific spot was subjected to. As reference, cholesterol (Chol) was subjected to five developments. Visualisation was done by sulphuric acid charring.

Four distinct spots were observed even after a single development with mobile phase. Resolution of the spots improved with consecutive developments with five developments providing optimal resolution for individual elution. The R_f values of the spots were (from bottom to top respectively) 0.37, 0.48, 0.62 and 0.73. Three of these spots are expected to be the subclasses α-, keto- and methoxy-MA (Laval *et al.*, 2001). Although the identity of the fourth (lowest) spot is unclear, it might represent unmethylated MA.

Laval *et al.* (2001) indicated that methylation was achieved with TMDM in an ethereal solution, but did not indicate the solvent composition of the solution. To analyse the effect of different solvent compositions of the methylation solutions as well as methylation's

effect on the mobility of other MA samples, a TLC was performed with self-prepared *M. tuberculosis* MA, commercial *M. tuberculosis* MA and *M. avium* MA methylated in either *n*-hexane or diethyl ether solutions of TMDM and compared to unmethylated samples (Figure 2.20).

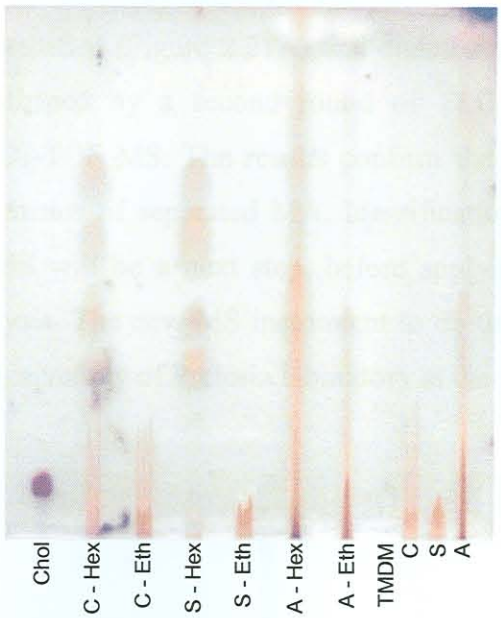

Figure 2.20: Separation of different diethyl ether or *n*-hexane methylated and unmethylated MA samples with five consecutive developments in 9:1 (v/v) petroleum ether:diethyl ether mobile phase. (Trimethylsilyl)diazomethane in *n*-hexane alone was spotted as a control along with cholesterol (Chol) as reference and visualisation was done by sulphuric acid charring. S – self-prepared *M. tuberculosis* MA, C – commercial *M. tuberculosis* MA, A – *M. avium* MA, Hex – *n*-hexane dissolved TMDM, Eth – diethyl ether dissolved TMDM.

Both the commercial and self-prepared *M. tuberculosis* MA methylated with the hexane dissolved TMDM showed resolved spots similar to those in Figure 2.19. *Mycobacterium avium* MA seemed to be too contaminated to be resolved. None of the unmethylated samples resolved beyond anything seen in previous experiments. All the MA samples incubated in the diethyl ether-dissolved solution of TMDM seemed to be unmethylated as no resolution of these samples occurred. No spot could be observed for TMDM alone indicating that all the spots observed were due to MA or contaminants remaining after isolation steps. As a result of this experiment it was determined that MA was successfully

separated into its different subclasses. Preparative separation of the MA followed by elution was now employed to prepare a source of separated MA subclasses.

2.4.1.11 Preparative thin layer chromatography of methylated mycolic acids

Self-prepared *M. tuberculosis* MA was striped, developed and visualised as described (*see* par 2.3.11). Spots were identified (Figure 2.21A) and eluted from the plate. Purity of the eluted fractions was confirmed by a second round of TLC (Figure 2.21B) and the remainder used for MALDI-TOF MS. The results confirm the success of the method to prepare pure samples by means of separated MA. Identification of the pure samples by means of MALDI-TOF MS will be a next step, before applying these pure samples as antigens in biosensor analysis. The new MS instrument to do this with was not, however, fully commisioned in the University of Pretoria laboratory at the time of going to print.

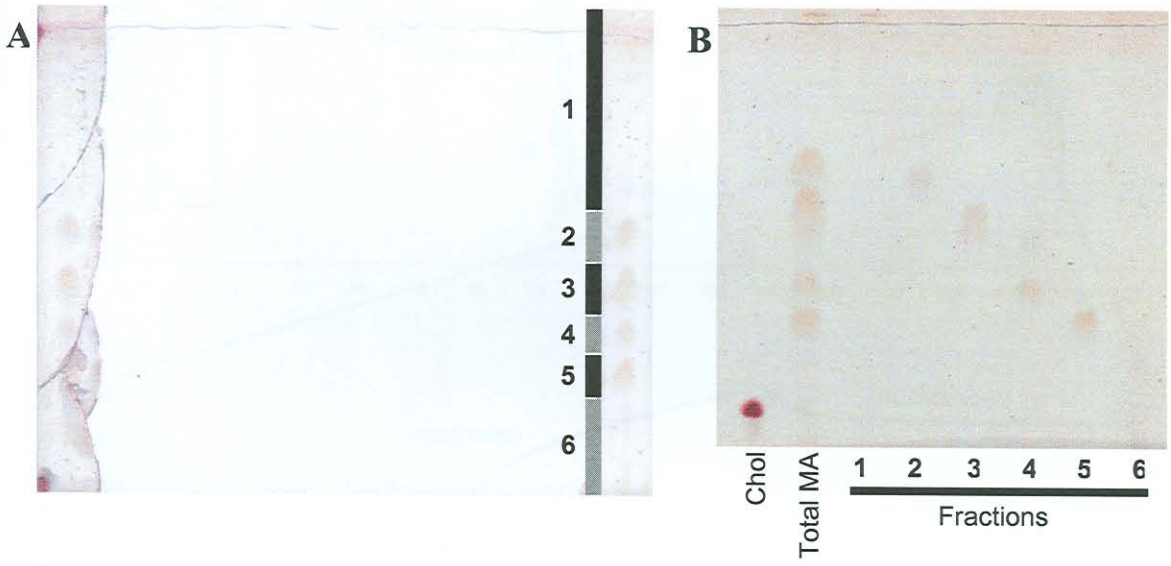

Figure 2.21A: Preparative TLC of methylated self-prepared *M. tuberculosis* MA. Fractions collected are numbered and vertical bars indicate the extent of collection. **(B)** Confirmation of purity of eluted methylated MA fractions. Visualisation was done by sulphuric acid charring.

2.4.2 Lipid antigen immobilisation on biosensor cuvette surfaces

2.4.2.1 Exploratory experiments with mycolic acid immobilisation on biosensor cuvette surfaces

A first experiment for the immobilisation of liposomes on non-derivatised IAsys cuvettes after activation with cationic detergent, performed according to the method innovated by G. Siko and J. Verschoor (Siko, 2002), gave a biosensorgram as shown in Figure 2.22A. The first peak and subsequent descent in signal was due to CPC activation of the surface.

The stable signal thereafter was obtained during a wash step with buffer. The response to liposomes being immobilised was variable and depended on the liposome concentration and constitution. The liposome immobilisation was followed by a brief wash step with buffer that stabilised the signal. A saponin 'blocking' step resulted in the sharp drop in signal that eventually stabilised. After another buffer wash step, the surface was ready for interaction analysis. Baseline was obtained in 25µl buffer, the test serum sample was added (25µl) and an association event was logged in the event log. Association was carried out over a predetermined time (here five minutes). The dissociation analysis was initiated with a wash step with buffer. Dissociation also continued over a predetermined time after which the cells were regenerated. In Figure 2.22B a typical interaction analysis is shown.

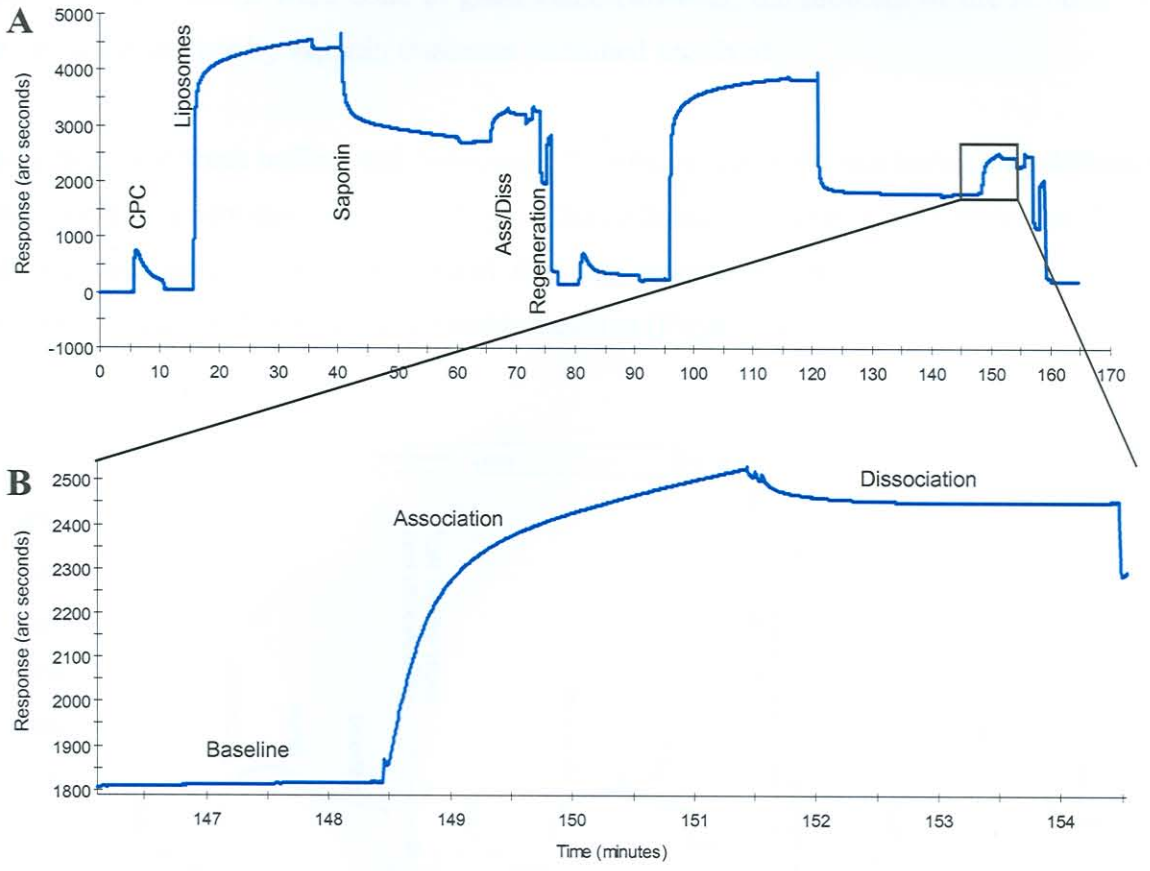

Figure 2.22: (A) A first IAsys biosensor interaction profile (biosensorgram) indicating the immobilisation of liposomes (10mg/ml) without MA, the association and dissociation of antibodies, and subsequent regeneration. **(B)** A magnification of the association/dissociation profile, showing the baseline, association and dissociation curves as recorded by the IAsys software.

Subsequent experiments were carried out with a liposome concentration of 10mg/ml or 500µg/ml not containing MA and a PC:cholesterol mass ratio of 2:1. Poor liposome binding followed by its removal during saponin wash steps were observed. Although MA-

liposomes showed a slightly better binding capacity than the empty liposomes (containing no MA), both liposome types were removed from the cuvette surface by the saponin treatment (not shown). Fresh stock solutions and new cuvettes could not improve the liposome binding capacity or prevent the immobilised layer from being removed by saponin.

It was suggested that plastic laboratory equipment used for liposome preparation might be responsible for poor results. Glass vials were used accordingly. Although liposomes prepared in glass vials had a better binding capacity, it still washed away with saponin treatment (not shown). Liposomes prepared in glass vials were tested on new cuvettes and reproducibly bound better than liposomes prepared in plastic tubes. All subsequent liposome preparations were done in glass vials. However, the problem of the removal of the liposome surface by saponin treatment remained unsolved.

Using the same fresh buffers and liposomes, the binding capacity was tested on a different biosensor and a new cuvette at the IAsys Affinity Sensors laboratory in Cambridge, U.K. Although successful, results suggested that the saponin treatment used to 'block' the liposome surface, still did not give a stable baseline (Figure 2.23).

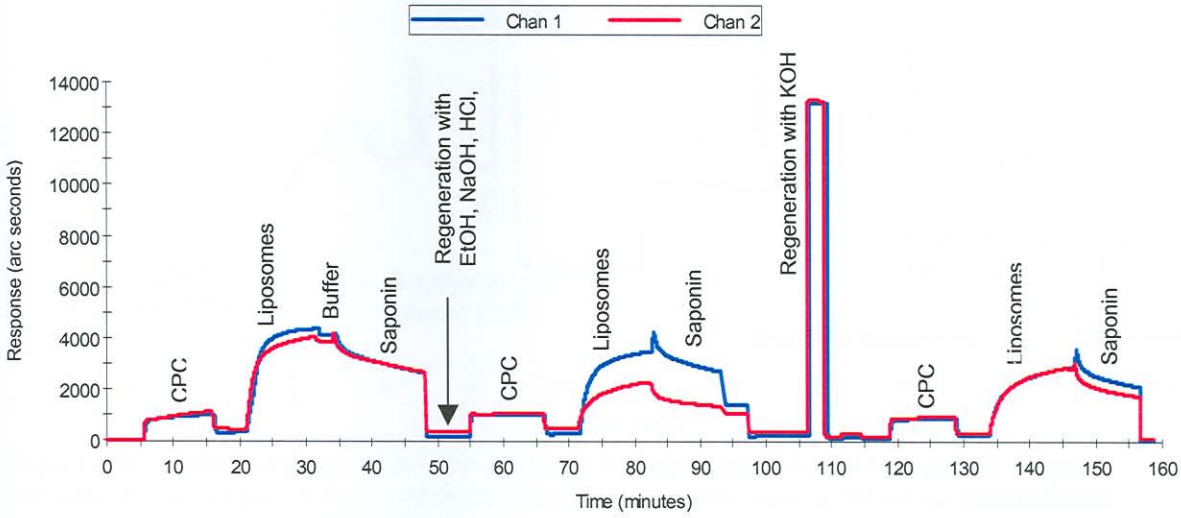

Figure 2.23: The biosensorgram obtained at the laboratories of IAsys Affinity Sensors, Cambridge, U.K. Uniform responses from both cells were achieved, baselines were stable, binding profiles were smooth and signals were high.

It was suggested that 12.5M KOH be used for regeneration instead of the complex steps used so far (personal communication, Paul Edwards, R&D Manager: IAsys, 2001) . The

extreme alkaline conditions created by the KOH wash step are believed to remove any excess fatty deposits and protein that might remain in a cuvette cell after interaction analysis. The KOH step showed promise as a regeneration method as the subsequent liposome immobilisation was stable and comparable between the two cells (Figure 2.23).

A third new biosensor was employed along with new cuvettes and 12.5M KOH as a standard regeneration method and gave comparable good results. The irreproducible results obtained on the three biosensor instruments using the identical reagents, buffers and solutions, suggested that the problem was to be found in the IAsys hardware of the first instrument. Although this was not followed up, possible problem areas could reside with oxidised stirrers or contaminated aspiration tubes. After several rounds of immobilisation and regeneration it was noticed that 12.5M KOH was not sufficient to remove everything from the surface of the cells. Ethanol was added to the protocol and Figure 2.24 shows that KOH alone does not regenerate the cell back to baseline but adding ethanol to the protocol does.

The sequence of first ethanol treatment and then KOH was subsequently found to be optimal (not shown).

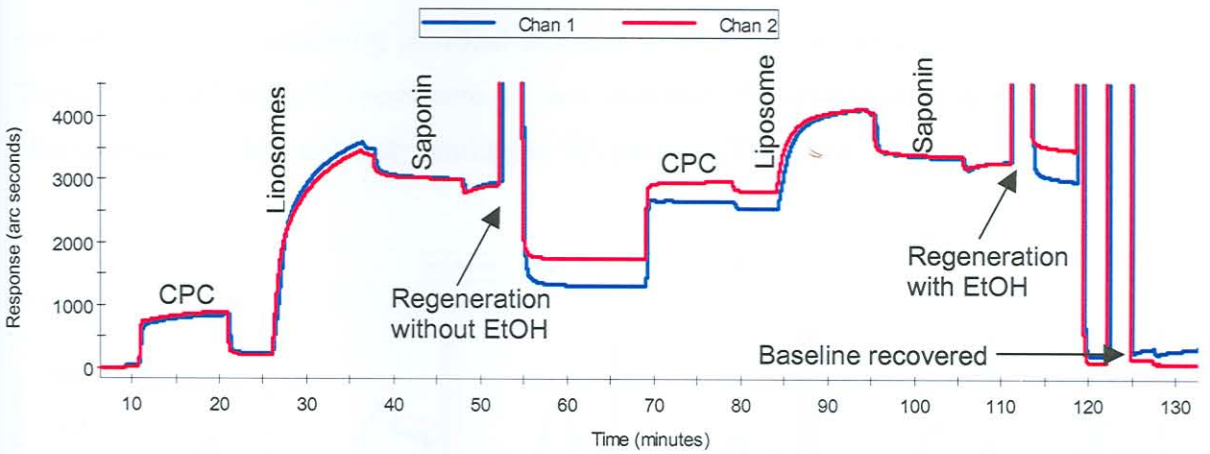

Figure 2.24: A biosensorgram showing the difference between regeneration with or without ethanol included. The sensorgram is representative of three identical experiments carried out on three different cuvettes, using liposomes at 500µg/ml.

2.4.2.2 Optimising mycolic acid-liposome concentration

With the regeneration method optimised, the MA-liposome concentration was titrated between 0.02mg/ml and 10mg/ml. The two channels, monitoring cell 1 and 2 respectively,

were taken as independent experiments and their extents of binding averaged in Figure 2.25. The MA-liposome concentration with the optimum binding capacity was found to be 500µg/ml and this concentration was used in all subsequent experiments.

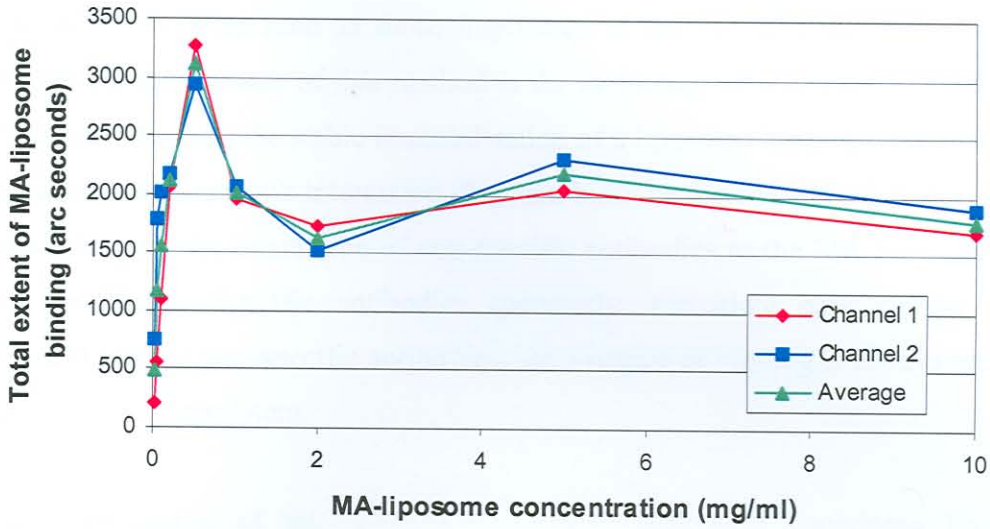

Figure 2.25: A titration of the optimal concentration of MA-liposomes for immobilisation on a non-derivatised biosensor cuvette. A concentration of 500µg/ml resulted in maximum liposome binding achieved in a biosensor measurement.

With the number of wash steps, incubation periods, CPC concentration, liposome concentration and saponin washing established, liposomes could be reproducibly immobilised on a non-derivatised surface, even when using liposomes prepared from separate aliquots containing identical amounts of PC, cholesterol and MA (Figure 2.26). This optimised method (Annexure 1) was successfully applied in a different study to characterise anti-MA antibody binding in TB patients (Thanyane, 2003).

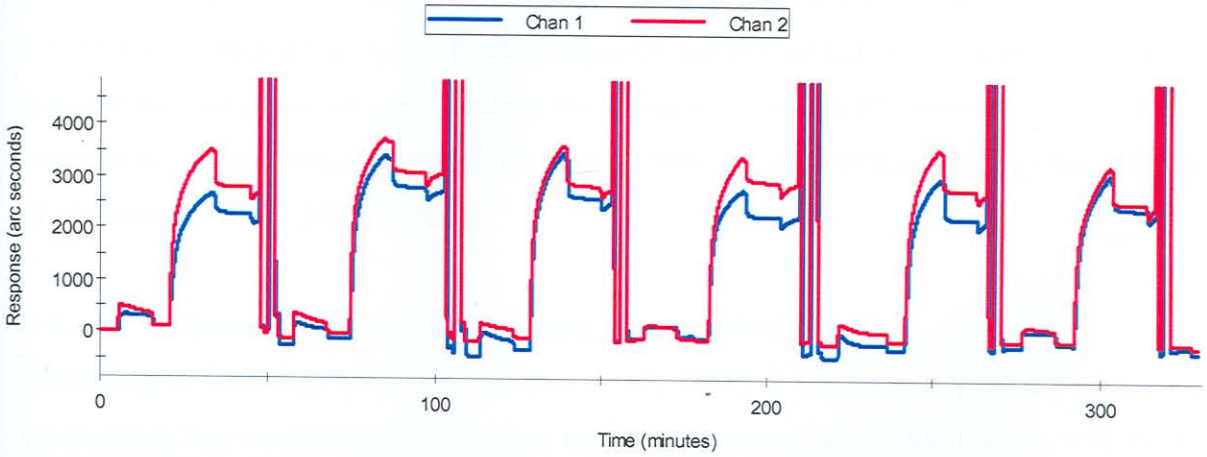

Figure 2.26: A biosensorgram to demonstrate reproducible immobilisation of separately prepared aliquots of MA-liposomes (500µg/ml) containing identical amounts of PC, cholesterol and MA in a non-derivatised IAsys biosensor cuvette.

2.4.2.3 *Application of method to ganglioside G_{M1}*

The method of immobilising MA-liposomes on a non-derivatised biosensor cuvette to analyse interactions of protein antibodies to lipid antigens is a novel application of the resonant mirror biosensor. The question arose whether this optimised method could be applied to other biolipids such as those implicated in the Guillain-Barré syndrome. As described above, the essence of this method is the activation of a non-derivatised surface with a cationic detergent, the stable immobilisation of a liposome layer and the blocking of this layer against non-specific interaction. Saponin binds to the cholesterol in the liposome membrane, blocking the interaction of non-specific antibodies to the MA imbedded in the liposome membrane. Specific antibodies apparently intercalate between the saponin molecules and replace non-specific antibodies, but a degree of binding is always seen when testing patient and control sera.

The wider application of this method was tested with G_{M1} containing liposomes, immobilised on a non-derivatised surface. Interaction analysis of G_{M1}-antibodies to G_{M1} was subsequently measured.

2.4.2.4 *Exploratory use of ganglioside-containing liposomes*

Based on initial trials with liposomes containing varying quantities of PC, cholesterol, MA and G_{M1}, it was observed that cholesterol generally added to the binding capacity of the liposomes (Table 2.1). The net binding capacities (calculated by subtracting the baseline response from the saponin treatment response) of different liposome compositions are listed separately for the two channels. Comparing the MA-liposomes (6PC:3Chol:1MA) to pure PC and empty liposomes (2PC:1Chol), it was concluded that MA and cholesterol had a synergistic effect on liposome binding capacity but MA added to PC alone (9PC:1MA), lowered the maximum possible binding. Including G_{M1} only in PC liposomes (9PC:1G_{M1}) lowered the binding capacity even further, but it was slightly elevated again by the addition of cholesterol (17PC:2G_{M1}:1Chol).

2.4.2.5 *Saponin is redundant when using ganglioside-liposomes*

According to literature (Athanassopoulou *et al.*, 1999) a blocking step is not necessary when using G_{M1} containing lipid bilayer surfaces. However, cholesterol along with PC in the liposome membrane appeared to enhance liposome immobilisation, and provide a target for saponin to stimulate blocking of non-specific ligand binding. Testing different

batches of saponin, it was found that batches are inconsistent in their activity. This could be due to the heterogeneity of saponin, a complex substance obtained from Quillaja bark, containing different sapogenins and monosaccharides. The age of the saponin could conceivably also make a difference due to different states of oxidation. The saponin did not contribute to attaining a stable baseline at 1mg/ml, as was observed in the MA-liposome coating, but instead washed away the G_{M1}-liposome coat. Experiments with G_{M1}-liposomes confirmed that even extensive washing with buffer only, after immobilisation, instead of 1mg/ml saponin, did not remove the liposome layer (Figure 2.27). It was decided to discontinue the use of saponin as a blocking agent. Cholesterol was employed at the start to have saponin bind to it for the purpose of blocking non-specific interaction. Since saponin was not being used anymore and blocking was shown to be redundant, it was decided to not include cholesterol in the liposomes anymore.

Table 2.1: Comparison of the net liposome binding capacities in an IAsys biosensor non-derivatised cuvette, using arbitrary compositions of PC, cholesterol, MA and G_{M1}.

Liposome composition	Channel 1 net liposome binding (arc seconds)	Channel 2 net liposome binding (arc seconds)	Average [(Chan1+Chan2)/2]
6PC:3Chol:1MA	2099	2073	2086
Pure PC	1493	1201	1347
2PC:1Chol	1290	1717	1504
9PC:1MA	1385	1097	1241
17PC:2G_{M1}:1Chol	1229	1215	1222
9PC:1G_{M1}	1143	883	1013

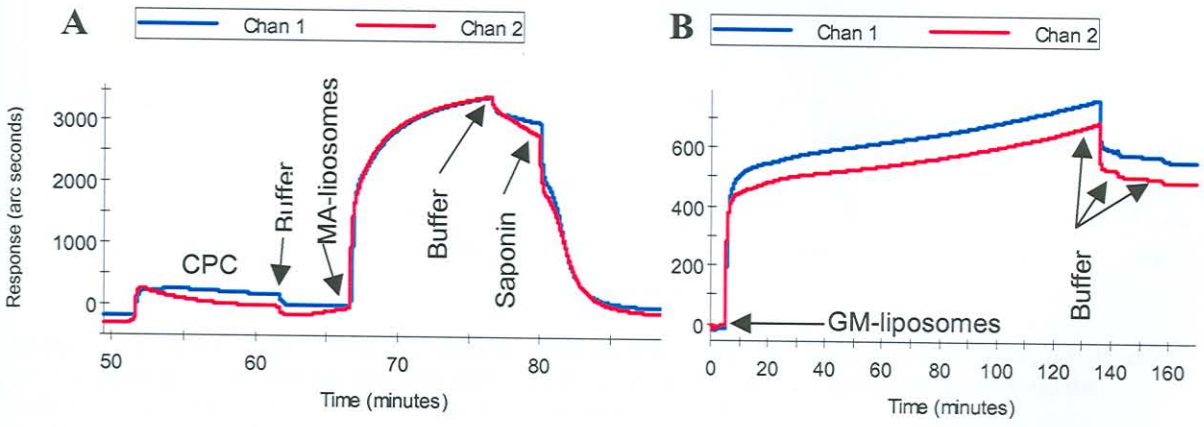

Figure 2.27: IAsys biosensorgrams demonstrating that successive wash steps with buffer do not remove an immobilised G_{M1}-liposome coat **(B)**, whereas a single treatment of saponin removes the MA-liposome coat **(A)**.

In the exploratory experiments a mass ratio of 6PC:3Chol:1G_{M1} was used following the optimised method for MA-liposome immobilisation (6PC:3Chol:1MA). This relates to PC,

cholesterol and G_{M1} molar percentages of 49.4%, 46.8% and 3.8% respectively. Molar ratios are the norm in publications and simplifies stoichiometric comparison.

2.4.2.6 Regeneration using ethanol/sodium hydroxide/hydrochloric acid

The continued regeneration of cuvettes after coating with G_{M1}-liposomes was found to be problematic. Progressively weaker binding of liposomes was observed, probably due to a cumulative etching effect of the surface during regeneration with 12.5M KOH during regenerations. As an alternative, NaOH and HCl were used in lower concentrations, as described by Altin *et al.* (2001). Briefly, three washes with 60µl 2M NaOH were performed after the ethanol washing step and followed by seven washes with 100µl water, three washes with 60µl 2M HCl and finally four washes with 60µl 20mM HCl. Besides being less harsh, improved liposome binding due to residual HCl remaining in the cuvettes before addition of subsequent liposomes was observed. Initial experiments with this method proved to be very successful in terms of the initial extent of liposome immobilisation, but the total binding capacity of G_{M1}-liposomes decreased with each re-coating (Figure 2.28).

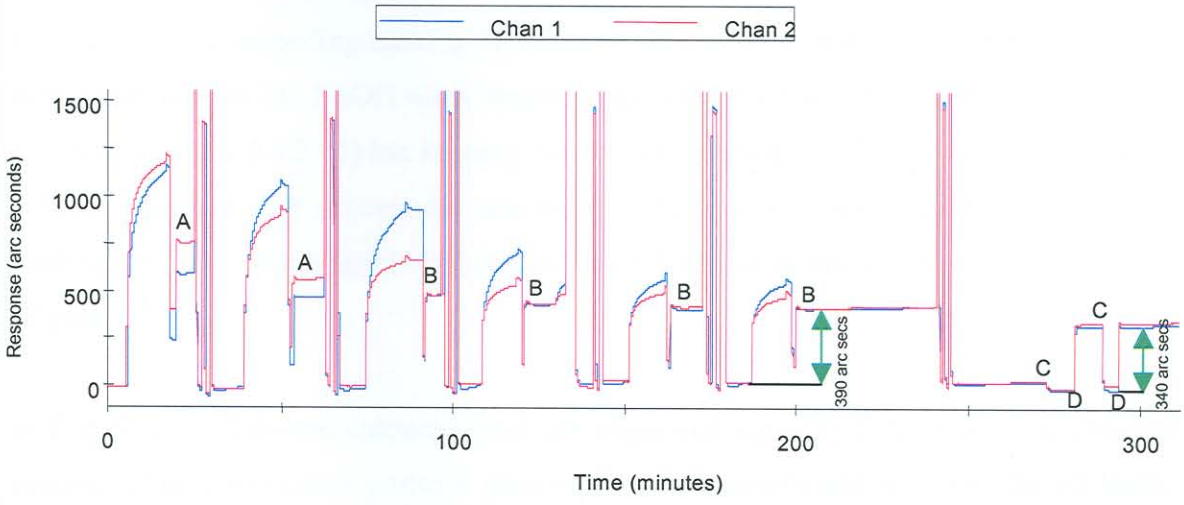

Figure 2.28: A biosensorgram of G_{M1}-liposome immobilisation and regeneration with ethanol, NaOH and HCl. Liposome coats were washed with either water or 10mM NaOH. The green arrows indicate the differences (arc seconds) in refraction indices between water and buffer.
A: Water wash step after G_{M1}-liposome immobilisation
B: 10mM NaOH wash step after G_{M1}-liposome immobilisation
C: Water wash step
D: Buffer (PBS/AE) wash step

After G_{M1}-liposome immobilisation, wash steps of either water (indicated by A in Figure 2.28) or 10mM NaOH (indicated by B in Figure 2.28) were included as was done by Altin *et al.* (2001). Cropped baseline levels were achieved with the 10mM NaOH wash steps, but not with the water wash steps. Subsequently, 10mM NaOH was used in all further experiments. The response (arc seconds) difference between buffer (PBS/AE) only (indicated by D in Figure 2.28), and water (indicated by C in Figure 2.28) was due to a difference in refractive indices of the two solutions. Comparing this difference (right green arrow), to the difference between baseline before and after liposome immobilisation (left green arrow), it was calculated that the net liposome binding was in fact only about 50 arc seconds (390-340 arc seconds). The response difference of 390 arc seconds is therefore not a true reflection of the G_{M1}-liposome binding capacity, as 340 of the 390 arc seconds can be ascribed to the difference in refractive indices of water and buffer.

2.4.2.7 Regeneration using ethanol/potassium hydroxide/hydrochloric acid

In a second experiment (not shown) good, reproducible liposome binding was attained using the method as described above, but subsequent binding of control serum to each new liposome coat, worsened progressively. It was thought that the 2M NaOH step in this new regeneration protocol (*see* par 2.4.2.6) was perhaps too weak to remove all of the protein from the surface, impeding ensuing experiments. It was decided to modify the regeneration method so that the 2M NaOH wash step be replaced by the harsher 12.5M KOH wash step as before (*see* par 2.4.2.11) but keeping the two HCl steps intact. This modification had the desired effect in that successive experiments showed not only reproducible liposome binding, but also reproducible binding of control serum to each new coat of liposomes (Figure 2.29).

In Figure 2.29, different coloured lines are sequential repeats of the same G_{M1}-liposome coating. This regeneration protocol gave reproducible results and was used for all further experiments.

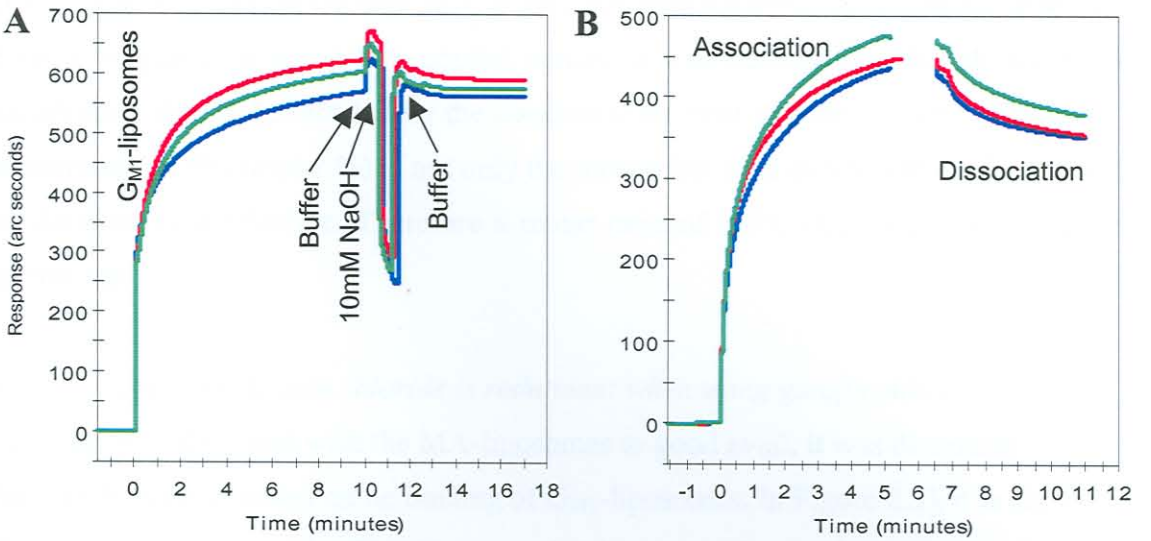

Figure 2.29: FASTplot overlays of sequential G_{M1}-liposome immobilisations and 10mM NaOH washing using ethanol, 12.5M KOH and HCl as regeneration solutions **(A)** and the subsequent association and dissociation of negative control serum **(B)**.

2.4.2.8 Ganglioside concentration optimisation

With other authors having used a range of 2-25% G_{M1} (molar percentage) for biosensor surface coating, it was deemed necessary to optimise the G_{M1} concentration. Three cholesterol-free liposome samples were used, containing respectively 5, 10 and 20% (molar) G_{M1}. The liposome binding capacities were fairly similar although a normal dose response was observed (Figure 2.30A). The association response of negative control serum to the three different surfaces were almost identical (Figure 2.30B).

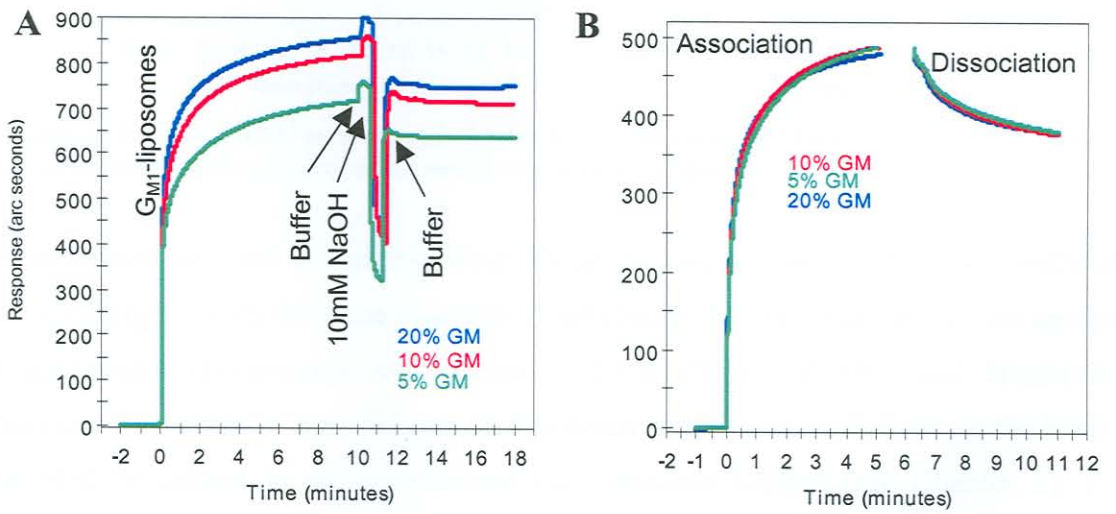

Figure 2.30: FASTplot overlays of G_{M1}-liposome immobilisations using three different G_{M1} concentrations (5, 10, 20%) and subsequent regeneration with ethanol, KOH and HCl **(A)**. The arrows indicate the different wash steps (Tris-buffer or 10mM NaOH) during liposome immobilisation. The negative control serum responses to the three different liposome coats were almost identical **(B)**.

With all three G_{M1} concentrations having the same binding capacity and more importantly the same response to a negative control serum, it was decided that the choice of G_{M1} concentration should be dictated by the concentration most popularly used in literature. A concentration of 5% (molar %) is not only the most often used in relevant publications, but also the most cost effective. Therefore a molar ratio of 19PC:1G_{M1} was used for further experiments.

2.4.2.9 Cetyl peridinium chloride is redundant when using ganglioside-liposomes

Since CPC was first used with the MA-liposomes to good avail, it was determined whether it had any beneficial effect on he binding of G_{M1}-liposomes. In Figure 2.31 it is shown that CPC does not enhance the G_{M1}-liposome binding capacity or the amount of negative control serum bound to the immobilised G_{M1}-liposomes. In fact, both are decreased by the presence of CPC.

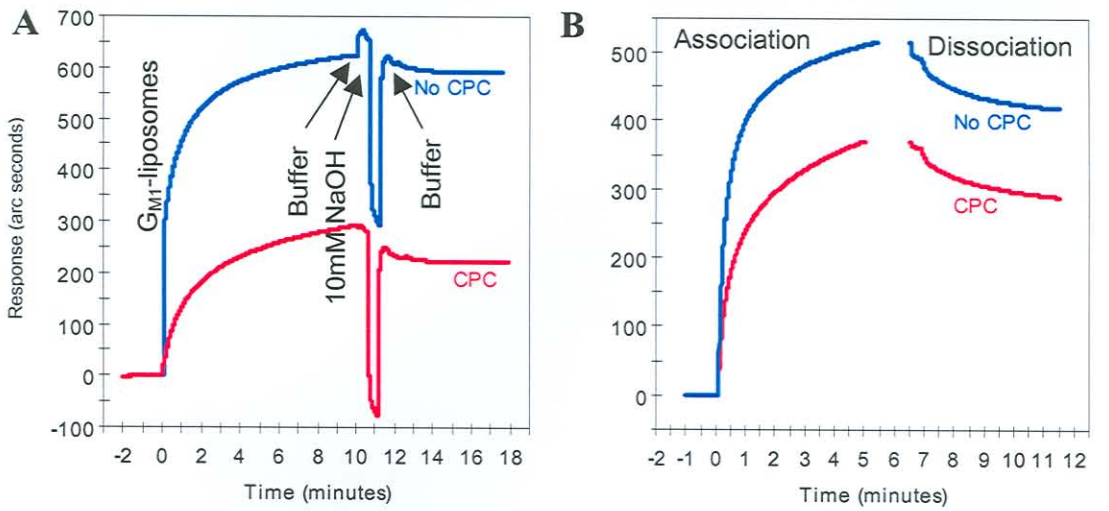

Figure 2.31: Effect of CPC on the immobilisation of G_{M1}-liposomes on IAsys biosensor cuvettes **(A)**, and subsequent negative control serum association to the G_{M1}-liposome coat **(B)**.

This optimised protocol of immobilising 500µg/ml G_{M1}-liposomes (5% G_{M1}) without a cationic detergent, stabilising the coat with 10mM NaOH before serum interaction analyses and subsequent regeneration with ethanol, 12.5M KOH, 2M HCl and 20mM HCl (Annexure 2) has been successfully applied to determine kinetic parameters for the binding of a positive control to an immobilised G_{M1}-liposome surface (*see* Chapter 3). It is expected that this method can be applied to obtain relevant kinetic data to discriminate between anti-G_{M1} antibody levels of different patients. This provides a tool to investigate

the role of such antibodies and their anti-idiotypic antibodies in the progression and recovery of GBS.

2.5 Discussion

2.5.1 The separation of mycolic acid subclasses with thin layer chromatography

In a study to determine the epitope specificity of IgG antibodies against cord factor (trehalose 6,6'-dimycolate, a monosaccharide containing two mycolic acids), it was shown that the antibodies distinguish between different subclasses of MA (Fujiwara *et al.*, 1999). This was confirmed in a follow-up study where a significant decrease in anti-cord factor IgG titre between *M. tuberculosis* cord factor and *M. avium* cord factor was observed (Pan *et al.*, 1999). The only difference between the two cord factors is the composition of the MA subclasses. This suggests that MAs are recognised as epitopes and that preferred subclasses are recognised by the antibodies in human TB patient sera.

The distribution of MA-subclasses in the cell wall determines the fluidity and therefore also the permeability of the cell wall (Liu *et al.*, 1996). Because MA-subclass composition has been linked to *M. tuberculosis*'s virulence in macrophages (Jackson *et al.*, 1999), it was suggested by these authors that the difference in virulence is not caused by different antibody profiles to different MA subclass compositions, but rather that the subclass composition determines the permeability of the cell wall and ultimately its virulence. Mycolic acids do, however, provide a unique footprint of *M. tuberculosis* and specific antibodies to one or more particular subclasses of MA may well turn out to be surrogate markers for tuberculosis infection (Pan *et al.*, 1999).

Moreover, the discovery of a structural mimicry between cholesterol and MA (Siko, 2002), first discovered as a cross-reactivity of tuberculosis patient antibodies to these compounds, emphasises the importance of determining the specificity of anti-MA antibodies against the various subclasses of MA. The biosensor is ideally suited to measure real-time affinities of ligates to ligands and subsequently to enable quantification of the antigenicities of the different subclasses of MA present in the cell walls of *M. tuberculosis*. This knowledge can be expected to contribute significantly to resolve the issue of the role of MA subclasses in the virulence of *M. tuberculosis*. The separation of MA into its subclasses for use in the biosensor would therefore be crucial to such research.

It is known that silver impregnated silica TLC plates can separate lipids in a single class differing only in the degree of saturation and the steric orientation of a double bond (Skipski & Barclay, 1969). This has been demonstrated by several laboratories (Kennerly,

1986; George *et al.*, 1995). In the publication by George *et al.* (1995), MA were radioactively labelled and applied to a TLC plate. The plate was developed twice into the $AgNO_3$-free strip with 19:1 hexanes:ethyl acetate, turned 90° and developed three times into the $AgNO_3$-impregnated part with 17:3 petroleum ether:diethyl ether. Plates were visualised and quantified with a Phosphor Imager to determine the quantities of each MA subclass. Initially, when applied in the current study, $AgNO_3$-impregnation was done by spraying a $AgNO_3$ solution onto a TLC plate and allowing it to dry. This method of $AgNO_3$-impregnation did not enhance separation, neither when TLC plates were submerged in $AgNO_3$ before separation as was done by George *et al* (1995). In fact, the MA did not move into the $AgNO_3$-impregnated region of the TLC plate at all. $AgNO_3$-impregnation of TLC plates was therefore abandoned.

All TLC analyses of the countercurrent purified MA samples showed a spot at the eluent front that did not contain MA. It is unclear what the nature of this contaminant is, but since all crude extracts went through the same initial purification steps, it is likely that the source of the contaminant originates from there. The mobile phases used here for all the experiments contained mostly hydrophobic organic solvents, so it is expected that the contaminant is also rather hydrophobic. It is likely that the spot may represent degradation products of fatty acids or alkanes formed during harsh saponification conditions or even countercurrent separation. Because it was shown that countercurrent purified MA preparations were pyrogen-free (Stoltz, 2002) and that the contaminant spot did not contain any MA, the matter was not investigated further.

Mycolic acids are considered to be neutral lipids as they don't contain any phosphorous or sugars in pure form (Skipski & Barclay, 1969). Due to this neutral character it was recognised that the introduction of a polar compound in the mobile phase, like acetic acid, might influence the separation. This increase in polarity of the mobile phase did not affect the mobility or the separation of the MA. Perhaps the non-polar nature of the MA is so overwhelming that polarity increase by adding an acid is irrelevant.

Mycobacterium avium, a slow grower like *M. tuberculosis*, has a slightly different MA TLC profile to *M. tuberculosis* (Kaneda *et al.*, 1986). Here it was shown to separate into three distinct spots, as opposed to *M. tuberculosis* MA that produces an unresolved smear. Unexpectedly, MA of *M. avium* did not separate into their different subclasses with the

20:80 diethyl ether:*n*-hexane mobile phase. Titration of the diethyl ether concentration demonstrated the possibility that a mistake was made by Kaneda *et al.* (1986) when they showed MA separation with 20:80 diethyl ether:*n*-hexane. Because MA is completely soluble in diethyl ether but only sparingly in *n*-hexane, it is to be expected that MA dissolves better in a higher diethyl ether concentration. Indeed, a mobile phase of 80:20 diethyl ether:*n*-hexane did increase the mobility of the MA even though it did not provide any resolution to the resultant smear.

In a different study, MA was methylated using TMDM after which separation on TLC was effected with five developments in a mobile phase consisting of 9:1 petroleum ether:diethyl ether (Laval *et al.*, 2001). The same method was successfully applied but the appearance of a fourth spot on the TLC profile was inconsistent with the results obtained by the authors. It is interesting that the R_f values obtained with the TMDM-methylated MA samples (between 0.37 and 0.73) correlate fairly well with the little resolved spots obtained by Kaneda *et al.* (1986) whose values ranged between 0.43 and 0.59. This suggests that the samples that Kaneda *et al.* (1986) separated must have been methylated as well. Inspection of their method indicates that they methylated their MA with methanol in the presence of sulphuric acid as an acid catalyst. Since it is not expected that the self-prepared MA used in this study are methylated at all, this observation explains the lack of mobility of MA during initial experiments. Similarly, the MA samples used in other publications were also methylated (George *et al.*, 1995; Yuan *et al.*, 1995; Yuan *et al.*, 1997). Methylation seem to be the only way to separate MA into their subclasses, but this might have implications for recognition by anti-MA antibodies in a biosensor set-up. If the methylated carboxylic acid group projects externally from the bacterial surface, methylation will decrease the affinity of antibodies to MA and biosensor experiments on TLC-separated MA will not reflect the true affinity differences. However, the separation on TLC of the methylated MA and its subsequent analysis in a biosensor is still a crucial step in determining the individual affinity constants of antibodies to the MA subclasses.

To analyse the identity of the different spots, mass spectrometry is employed. Electron-impact mass spectrometry has been successfully employed previously for the elucidation of MA structure (Dubnau *et al.*, 1997; Quémard *et al.*, 1997), but although this technique provides important information about MA structure, the fragmentation patterns caused by pyrolysis are complex due to the presence of homologues and the loss of water and

methanol from the native molecules (Laval *et al.*, 2001). Initial experimentation with EI-MS supported these findings. It was decided to attempt the more sensitive MALDI-TOF MS technique (Laval *et al.*, 2001) in future.

It was concluded that MA subclasses are separable with the methods described (George *et al.*, 1995; Yuan *et al.*, 1997; Watanabe *et al.*, 2001), but preparative isolation of the subgroups is expensive and very difficult. Pending the outcome of the analysis of the different bands of the separated MA, a decision can be made as to the useful testing of these fractions in the biosensor to determine the specificities of binding of TB patient antibodies. In the meantime the biosensor method for immobilising MA-liposomes was optimised and tested for application to the GBS disease model.

2.5.2 Immobilisation of lipid antigens on a biosensor cuvette surface

Protein-protein interactions are well defined and their interaction characteristics have been successfully determined with optical biosensors (Boulla *et al.*, 2000). These interactions were usually measured between proteins in solution and proteins on an immobilised surface. Broadening the application field, interactions between molecules in solution and their transmembrane protein receptors in their native environment have also been measured (Nikolelis *et al.*, 1999). This was done by creating artificial bilayer membranes on the surface of the biosensor with the transmembrane proteins imbedded in the bilayer. Expanding even further, studies have shown that it is possible to study interactions between the lipids of an artificial immobilised bilayer and ligands in solution (Altin *et al.*, 2001). Now a new field is emerging: characterisation of antibody binding properties to lipid and glycolipid antigens immobilised in liposomes on a biosensor surface.

The method for liposome immobilisation on a cationic detergent (CPC) activated sensor surface (Siko, 2002) worked well, but regeneration was optimised to include a concentrated KOH wash. Mycolic acids in the pure form consist of lipid only. Part of the waxy tail is imbedded in the membrane and the part that protrudes from the membrane is antigenic. This implies that the surface of the MA-liposomes probably retain some hydrophobic character, leading to the enhanced liposome binding possible with MA-liposomes on a CPC activated surface.

Perhaps due to an etching effect caused by the corrosiveness of the high KOH concentration, the cuvette surfaces deteriorated progressively throughout experiments. Maximally forty rounds of immobilisation, interaction analysis and regeneration could be achieved per cuvette.

Ganglioside G_{M1} had been immobilised in combination with PC before (Athanassopoulou *et al.*, 1999) and also as G_{M1}-liposomes (MacKenzie *et al.*, 1997). Athanassopoulou *et al.* (1999) utilised the standard hydrophobic cuvettes available to IAsys biosensor users. Although useful for certain studies, this method was found to be ineffective for MA immobilisation and abandoned (Siko, 2002). To our knowledge, a resonant mirror biosensor has never been used before for immobilising MA- or G_{M1}-liposomes on a non-derivatised surface.

There is a marked difference in the immobilisation protocols between MA-liposomes and G_{M1}-liposomes. It is shown here that CPC activation at the cuvette surface is not required for G_{M1}-liposome immobilisation. This is probably due to the polysaccharide moiety of G_{M1} gangliosides. Ganglioside-liposomes have a hydrophilic surface created by the glycosilated gangliosides. The hydrophilic liposome surface should be able to associate with a hydrophilic cuvette surface without the activation with cationic detergent.

Blocking of non-specific interactions has been shown to be redundant for G_{M1} (Athanassopoulou *et al.*, 1999). A matter that complicates the qualitative as well as quantitative determination of kinetic MA-antibody binding parameters, is the cross-reacting cholesterol antibodies found in varying levels in the sera of all humans (Alving & Wassef, 1999). With the antigenic properties of cholesterol, one would expect a certain degree of interaction with antibodies on liposome surfaces containing cholesterol. The stabilising effect of cholesterol on liposomes, especially when they contain MA, makes for a difficult choice whether to include cholesterol or not. If cholesterol could not be excluded, it would become necessary to block such surfaces from interactions not specific to MA. As saponin is specific to cholesterol, it would seem the ideal way of blocking MA-liposome surfaces.

Regenerations between the two surfaces also varied. It appeared to be necessary to neutralise the harsh alkaline conditions during regenerations when using G_{M1}-liposomes

but not MA-liposomes. It is possible that because G_{M1}-liposomes associate so much easier with the cuvette surface than MA-liposomes, they require less harsh conditions to remove. Even so, it has been shown that not having the harsh alkaline conditions, lessens the reproducibility of subsequent experiments in the same cuvette.

In the literature, concentrations of 2-25% G_{M1} have been used to determine cholera toxin (CTx) binding affinities (Masserini *et al.*, 1992; Kuziemko *et al.*, 1996; MacKenzie *et al.*, 1997; Athanassopoulou *et al.*, 1999). Although indicative of typical G_{M1} biomembrane concentrations, some of the experiments using 2% G_{M1} were unsuitable for the biosensor application. In one study it was shown that 25% G_{M1} reaches maximal binding capacity (Athanassopoulou *et al.*, 1999). However, this immobilisation was done on hydrophobic IAsys cuvettes with a different chemical immobilisation principle than used here. Kuziemko *et al.* (1996) determined that the lowest G_{M1} concentration that gave analysable kinetic data was 5% (molar %). Therefore the concentration of 5% G_{M1} seemed most logical and cost effective.

In a BIAcore biosensor, utilising surface plasmon resonance, *Salmonella* LPS imbedded into liposomes that contained different gangliosides, were captured with anti-LPS IgG immobilised on a CM5 sensor chip containing a CMD matrix similar to CMD surfaces of IAsys cuvettes (MacKenzie *et al.*, 1997). This complex set-up apparently created an artificial lipid bilayer of PC and gangliosides on the sensor chip surface and was used to determine kinetic parameters for cholera toxin B-subunit (CTxB) binding to gangliosides. It was determined that this set-up is too complex and not relevant for use in the IAsys biosensor. Kuziemko *et al.* (1992) also utilised a BIAcore biosensor, but successfully employed a method much similar to the optimised method used here for MA-liposome immobilisation. CM5 sensor chips were stripped completely of their CMD matrices to produce non-derivatised surfaces. Octadecylmercaptan (ODM) was used to activate the surface similar to CPC, after which a lipid solution (resembling liposomes) was added to create a self assembled bilayer.

Taken together, all these experiments indicate that there are different biosensor immobilisation methods available for different purposes and that they are not universally applicable. That has also been confirmed in this study with a different set-up needed for G_{M1}-liposome compared to MA-liposome immobilisation. The ultimate aim would be to

optimise a method for a specific purpose so that it is cost-effective, fast and optimal in terms of result output.